Fall 2015

THE INFLUENCE OF CENTRAL THALAMUS ON CODING PROPERTIES OF PREFRONTAL CORTEX

Benjamin Aaron Wormwood
University of New Hampshire, Durham

THE INFLUENCE OF CENTRAL THALAMUS ON CODING PROPERTIES OF PREFRONTAL CORTEX

BY

BENJAMIN A. WORMWOOD

B.A. Ithaca College, 2007

M.A. University of New Hampshire, 2012

DISSERTATION

Submitted to the University of New Hampshire

in Partial Fulfillment of

the Requirements for the Degree of

Doctor of Philosophy

In

Psychology

September, 2015

This thesis/dissertation has been examined and approved in partial fulfillment of the requirements for the degree of Doctor of Philosophy in Psychology by:

Dissertation Director, Dr. Robert G. Mair, Professor of Psychology

Dr. Robert C. Drugan, Professor of Psychology

Dr. Brett M. Gibson, Associate Professor of Psychology

Dr. Wayne J. Smith, Senior Lecturer, Electrical and Computer Engineering

Dr. Winsor H. Watson, Professor of Zoology

On July 16, 2015

Original approval signatures are on file with the University of New Hampshire Graduate School.

DEDICATION

This work is dedicated to my wife, Jolie. Without her incredible patience, love and support, none of this would have been possible.

ACKNOWLEDGEMENTS

I would like to thank the members of my committee for their hard work and support, especially my adviser and committee chairman Dr. Robert Mair, who has served as a mentor throughout my career at UNH and was integral in the development of my current research. I would like to thank Dr. Robert Drugan and Dr. Brett Gibson, who were teachers and practicum advisers in addition to volunteering their time to work on my committee. I would also like to thank Dr. Wayne Smith and Dr. Win Watson, who worked outside their respective departments to aid in the development, conduction and evaluation of years of research on this project.

I would also like to thank the graduate students who worked with me toward this goal. Dr. Kristen Onos and Dr. Jackie Short (née Hembrook) first welcomed me into the lab and helped me transition into graduate research. Dr. Onos remained for several years training me and offering invaluable assistance in everything from research to coursework to my teaching, and has been a friend and mentor during my work here. Rikki Miller has been a friend and fellow cohort member since we began our graduate work, and has been essential in helping me to complete this research. I would also like to thank Miranda Francoeur and Dylan Chase, who joined our lab as undergraduates and have gone on to be promising and dedicated graduate researchers, from whom I expect great things.

Finally I would like to thank all of the incredibly motivated and hard-working undergraduate research assistants that helped make this work possible, especially those most directly involved in my projects, including (in alphabetical order) Drew Blake, Erica Brasley,

Austin Drake, Candice Ellis, Liz Hebert, Cora Lehet, Lydia Manzo, Joe McKee, Ted Kazan, and Hayley Robertson.

This research was made possible in part by a UNH Research Leverage Initiative Grant, for which I am extremely grateful, as well as two Summer Research Fellowships which helped me continue my work between semesters.

TABLE OF CONTENTS

List of Tables

List of Figures

ABSTRACT

THE INFLUENCE OF CENTRAL THALAMUS ON CODING PROPERTIES OF PREFRONTAL CORTEX

by

Benjamin A. Wormwood

University of New Hampshire, September, 2015

Medial thalamus has reciprocal connections with prefrontal cortex (PFC) that are thought to coordinate its activity with other areas of the telencephalon that support flexible goal-directed behavior. The mediodorsal nucleus is the primary source of specific thalamo-cortical projections to middle layers of PFC while midline and intralaminar nuclei provide modulatory inputs to deep and superficial layers of PFC and to anatomically-related areas of the basal ganglia and hippocampus. Each of these nuclei receive direct cortico-thalamic and indirect cortico- striato-pallidal input from PFC. Medial thalamic lesions impair flexible goal-directed behavior, exemplified by delayed non-matching to position tasks (DNMTP).

To elucidate the influence of medial thalamus on PFC function we examined the effects of temporary thalamic inactivation on the response properties of prefrontal neurons in rats performing a dynamic DNMTP task. Cellular activity was recorded throughout medial PFC using a drivable array of tetrodes. Electrophysiological recordings were analyzed offline to identify signals from isolated neurons and to correlate activity with specific behavioral events as rasters and peri-event time histograms (PETH).

Once cells with significant behavioral correlations (PETH responses beyond 99% confidence interval) were identified (day 1), the tetrode array was left in place for two more sessions. On the next day (day 2), central thalamus was unilaterally inactivated using microinjections of the $GABA_A$ agonist muscimol. On day 3, activity in the same location was recorded again without thalamic inactivation. We used doses of muscimol previously shown to impair delayed matching to position when injected bilaterally at the same site. Unilateral inactivation had no significant effect on DNMTP performance.

Examination of waveforms, inter-spike-interval histograms, cluster analyses, and event related activity (on days 1 and 3) confirmed the identity of single neurons across the three days. Day 2, inactivation was consistently associated with significant disruption of event-related activity of prefrontal neurons, but not with significant changes in performance accuracy or mean firing rate of cells. Some neurons exhibited increased and others and decreased levels of activity, suggesting both inhibitory and excitatory modulation of PFC by thalamus. These data indicate a critical role for medial thalamus in shaping the activity of cortical neurons in relation to memory dependent responding and goal directed action.

INTRODUCTION

All memory involves the storage and retrieval of information drawn from experience. The ability to build rich and productive lives as humans derives largely from our ability to store and process an incredible amount of information constantly. While ingrained in every aspect of daily life and thus often taken for granted, the breakdown of our ability to store and accurately retrieve memories can have global and devastating effects on one's life. Without intact memory one loses the ability to navigate the environment, to attend to the relevant stimuli in a given situation, and even the sense of self and one's connection to friends and family can slowly fall apart.

Our memories are a product of a vast and interconnected system of discrete brain regions cooperating in the encoding and retrieval of experience, representing changing knowledge in terms of altered patterns of activity among the billions of neurons in the human brain. While new information is always emerging to describe these interconnected systems, two key regions already stand out as being closely tied to memory function, albeit among other functions. These regions are prefrontal cortex (PFC), a region located in the anterior portion of the frontal lobe shown to be critical in processes ranging from attention to emotion regulation to executive function and conscious control of actions in humans and even some other species (Miller, Freedman, & Wallis, 2002).

Another critical region in the processing of memory is the thalamus, damage to which is associated with severe cases of amnesia (Winocur, Oxbury, Roberts, Agnetti & Davis, 1984). This points to the region's importance in storing and retrieving information, but neither the

thalamus nor prefrontal cortex alone could account for the complexity of human memory and the actions we perform based on that memory. In fact, the two regions are densely connected to one another, communicating back and forth via a network of direct neural pathways as well as indirect connections involving other intervening brain systems (Hoover & Vertes, 2007). Recent evidence suggests that, in rats, PFC is dependent on input from the thalamus for the successful solution of certain memory tasks, illustrating the importance of communication between PFC and thalamus (Floresco, Braaksma, & Phillips, 1999).

The functions performed by these critical regions, as well as the complex tasks which rely on the interplay of the two, will be the focus of this investigation, with the goal of characterizing the patterns of neural activity which underlie these memory processes.

CHAPTER 1

Role of Prefrontal Cortex in Executive Function and Working Memory

The prefrontal cortex is found within the frontal lobe of the brain in mammals, and is particularly well developed in humans, who possess one of the largest frontal lobes relative to other brain areas. This anatomical observation, along with the unique abilities which humans possess over other mammals, supports the notion that our frontal lobes are at least one essential piece of what makes us human. This idea is supported by decades of research which support the role of the frontal lobe, and prefrontal cortex in particular, in complicated tasks ranging from attention and visual discrimination (Rafal & Posner, 1987) to deductive reasoning (Goel, 2007) and emotion (Cardinal, Parkinson, Hall, & Everitt, 2002). Damage or dysfunction in PFC has been found to cause disruption in some or all of these functions, pointing to just how essential this part of the brain is to tasks relevant to everything from daily survival to deeper intellectual pursuits.

PFC appears essential for planning and goal-directed action (Miller, Freedman, & Wallis, 2002). And it is this role which involves PFC in working memory processes, using active representations of experienced stimuli to direct effective courses of action.

Within prefrontal cortex, the areas oriented along the midline of the mammalian brain, known as medial prefrontal cortex (mPFC) seem to be most closely tied to memory processes. Crucially, this is also a region which has dense connections with thalamic nuclei also show to participate in memory tasks, and it would be a mistake to think that these aspects of mPFC are unrelated (Hoover & Vertes, 2007). Anatomical research has broken mPFC into four major

regions: medial (frontal) agranular (AGm), anterior cingulate (AC), prelimbic (PL), and infralimbic (IL) cortices (Hoover & Vertes, 2007). These areas have been determined using common characteristics among cell populations, usually relying on morphology or cytoarchitecture as unifying features, although there is still some disagreement as to where exactly the borders among regions lie (Wilson, Gaffan, Browning & Baxter, 2010). Working with these limitations, distinct functions can still be found for the discrete areas of mPFC. The more dorsal regions of mPFC, AGm and dorsal parts of AC, are innervated largely by sensorimotor areas in cortex, in turn sending afferent projections to motor systems in nearby neocortical areas (Hoover & Vertes, 2007; Devsinky, Morrell & Vogt, 1995). This suggests that the role played by dorsal mPFC is distinct from its more ventral nuclei, and that this role is likely closely tied to sensation and voluntary action, while also being linked to functions as diverse as coping processes involved with evaluating controllable stressors and coping accordingly (Amat et al., 2005). This idea is borne out by research linking AC disruption, due to epilepsy in humans or experimental manipulations in animals, to disorders of motor control as well as, interestingly, emotion regulation (Devsinky, Morrell & Vogt, 1995). AC has also been linked, along with the more ventral prelimbic and infralimbic cortices, to processes involved in spatial working memory and navigation (Dias & Aggleton, 2000; Ragozzino, Adams, & Kesner, 1998), with lesions to these areas negatively impacting learning of delayed matching tasks and interfering with behavioral flexibility. This suggests all of these regions may be involved in the inhibition of prepotent response impulses during the learning and performance of memory dependent tasks.

The more ventral sections of mPFC, PL and IL, have dense connections to subcortical structures in the limbic system, a circuit with well-supported functions involving spatial and working memory (Hoover & Vertes, 2007). The limbic system consists of a network of

subcortical structures including the hippocampal formation and amygdala, both known to perform a number of memory functions, with hippocampus being critical for spatial representation as well as contextual and spatial memory, and amygdala being tied to the experience of emotions as well as the encoding of emotionally charged memories (Morgane, Galler & Mokler, 2005). In addition to its indirect involvement in emotion and memory, ventral mPFC is also involved in stress reactivity via its excitatory projections to the Dorsal Raphe Nucleus, suggesting a broader role in many types of memory, including learned responses to stressors, likely with their own emotional component (Amat et al., 2005). Thus it is not surprising that the areas of mPFC which seem to be necessary for successful completion of memory-dependent tasks are also those which have the most connections with other systems known to participate in working memory.

Previous studies examining prefrontal cortex have shown that reversal learning was only impaired when stimuli were difficult to discriminate (Bussey, Muir , Everitt & Robbins, 1997) and it is possible that impairment was caused by the lack of being able to attend to the features of the stimulus. Birrell and Brown (2000) induced lesions in medial prefrontal cortex using ibotenic acid and found no impairments in the acquisition of a reversal learning task involving odor/texture discriminations. Conversely, Chudasama and Robbins (2003) found that lesions of the infralimbic cortex increased the number of sessions that were required to reach criterion during the learning of the reversals. These data make the specific role of mPFC in memory somewhat less clear, as if it is in fact crucial to reversal learning it may be tied to general processes of simple rule learning by classical conditioning. On the other hand, if future results indicate a specific deficit only during delay periods, a more narrow definition of the region as critical to working memory may in fact be appropriate. Given the existing evidence, however, it

seems likely that the area plays at least some part in maintaining memory traces during delay periods.

Chang and colleagues (2002) have analyzed neuronal activity in PFC of rats performing a working memory task, reporting that medial PFC activity is increased during delays when animals must hold information in working memory in order to respond at the end of a memory delay. This evidence suggests that the cells in mPFC are involved in the maintained representation of information over a delay period. This sustained cellular activity in the absence of stimulation indicates that the cells are coding memory during task performance. Rich and Shapiro (2009) have also demonstrated changes in the activity of neurons recorded in the prelimbic and infralimbic areas of medial PFC related to rats changing response strategies based on working memory. These regions of prelimbic and infralimbic cortex in rats have been found to have specific importance to tasks relying on visual spatial memory (Eichenbaum, Clegg & Feeley, 1983), and are thought to be homologous to the dorsolateral prefrontal cortex of non-human primates like the Rhesus macaque, a region which is found in monkeys to show delay-period activity much the way IL and PL have done in rats (Funahashi, Bruce & Goldman-Rakic, 1989).

Together these data point to medial prefrontal cortex, and infralimbic and prelimbic cortices specifically, as key sites of memory coding activity in the rat brain. These regions, in addition to displaying these properties on their own, also show dense connections to central thalamic nuclei, which play their own role in memory-related processing in addition to influencing the function of mPFC.

CHAPTER 2

Role of Central Thalamus in Memory and Cognition

Central thalamus has been shown to be critical to memory processes as well as the regulation of alert, wakeful states. Damage to thalamus is associated with severe memory dysfunction, including global amnesia in humans as well as analogous symptoms in monkeys (Zola-Morgan & Squire, 2004). Lesions to the midline nuclei in central thalamus, specifically, have produced significant memory deficits in non-human primates as well, including difficulty with recognition memory (Aggleton & Mishkin, 1983). Recent research also indicates that, while inactivating thalamus impairs cognitive function, increasing activity in thalamus can actually improve the function of working memory (Shirvalkar, Seth, Schiff, & Herrera, 2006). These data indicate a major role of thalamus in working memory, in particular central nuclei within the area. However, the connections these nuclei make throughout the brain may be just as essential to their function. It is possible that a major part of central thalamus's function in working memory has to do with its myriad connections to cortical and subcortical structures performing their own memory coding.

Two areas of the brain known to be important in working memory processes are prefrontal cortex and hippocampus (Yoon, Okada, Jung & Kim, 2008; Wang & Cai, 2006). The hippocampus has strong connections to medial prefrontal cortex, but there are no direct return projections from medial prefrontal cortex to hippocampus (Thierry, Gioanni, Degenetais & Glowinski, 2000; Vertes, Hoover, Szigeti-Buck & Leranth, 2007). This suggests the presence of another brain structure that acts as an intermediary between these two structures to facilitate this

communication. Anatomical studies suggest that central thalamus, and specifically two ventral midline thalamic structures, the reuniens and rhomboid nuclei, may be the critical link between medial prefrontal cortex and hippocampus (Viana, DiPrisco & Vertes, 2006, Vertes et al. 2007).

Setting aside meaningful connections with hippocampus, central thalamic nuclei are also important sources of thalamocortical projections which have been implicated in the control of arousal, attention and awareness (Jones, 1985; Steriade, Jones & McCormick, 1997; Van der Werf, Witter & Groenewegen, 2002). Clinical studies have linked damage to these nuclei with cognitive deficits affecting attention, memory and motor function and other aspects of executive functioning (Zola-Morgan & Squire, 1993; Braak & Braak, 1998; Gold & Squire, 2005) as well as deficits in awareness observed with coma, persistent vegetative state and akinetic mutism (Schiff, 2008).

The midline and intralaminar thalamic nuclei were previously described as 'nonspecific' (Jones 1985, Groenewegen & Berendse 1994, Van der Werf, Witter & Groenewegen, 2002) due to the varied efferent projections to multiple populations of prefrontal cells (Jones & Leavitt, 1974). Studies which applied excitatory electrical stimulation to intralaminar nuclei resulted in widespread changes in cortical activity (Dempsey & Morison, 1942; Moruzzi & Magoun, 1949; Jasper, 1960). These data would seem to suggest a broad and ill-defined role for central thalamus in working memory, but more recent evidence suggests there may be more defined communication between PFC and thalamus.

Tracing techniques have identified anatomical connections among these key regions. Four major groups of midline thalamic nuclei have been identified based on this research: the lateral, the dorsal, the ventral medial, and the posterior group. These different groups potentially play different roles in brain functioning and patterns of connectivity. The lateral cluster consists

of the anterior central medial, paracentral and central lateral nuclei (Van der Werf, Witter & Groenewegen, 2002). This cluster projects to areas in mPFC along with the medial striatum. This area has been shown to play an important role in executive functions including aspects of attention, working memory, and decision making (Shallice, 1982; Baddeley & Della Sala, 1996). The posterior intralaminar cluster includes the centre median (found in primates but not rats) and parafasicular nuclei and has robust connections with the basal ganglia. This cluster has limited cortical projections, primarily to the lateral agranular areas in the rat corresponding to primary and secondary motor cortex. These connections suggest a role related to the planning and execution of responses as well as aspects of motor control (Burk & Mair 2001; Mair, Koch, Newman, Howard & Burk, 2002; Hembrook & Mair, 2010). The ventral medial cluster consists of the rhomboid, reuniens and posterior central medial nuclei. This cluster has inputs to the hippocampus and parahippocampal cortex, two areas shown to be heavily involved in spatial memory, indicating a possible role for these nuclei in related processes (Van der Werf, Witter & Groenewegen 2002; Hembrook & Mair, 2010).

Hippocampus sends strong projections to medial prefrontal cortex and has strong excitatory actions here, but there are no direct efferent pathways returning from medial prefrontal cortex to hippocampus (Hoover & Vertes, 2007). Recent anatomical work by Vertes and colleagues (2007) suggest that reuniens (Re) and rhomboid (Rh) nuclei may represent a critical link between medial prefrontal cortex and hippocampus. Re was the only nucleus of the thalamus where fibers from medial prefrontal cortex and hippocampus showed strong convergence (Vertes, Hoover, Do Valle, Sherman & Rodriguez , 2006; Vertes, Hoover, Szigeti-Buck & Leranth, 2007).

Both Re and Rh have projections to prefrontal cortex and the hippocampal system (CA1 and subiculum). However, Re is unique because medial prefrontal cortical fibers connect with the dendritic shafts of neurons in Re which directly project to hippocampus (Vertes et al., 2006). This research, as well as studies using electrical microstimulation, (Dolleman-Van der Weel, Lopes da Silva & Witter, 1997; Viana DiPrisco & Vertes, 2006), implies connections between the structures would form a loop through reuniens: CA1/subiculum to medial prefrontal cortex to Re and then back to CA1 (Vertes, Hoover, Szigeti-Buck & Leranth, 2007).

Based on their projections to prefrontal cortex and hippocampus, both Re and Rh are hypothesized to be important for spatial working memory. However, Re has the unique attribute of receiving input from prefrontal cortex that terminate on neurons which project directly to hippocampus (Vertes et al. 2006), leading some (Dolleman-van der Weel, Morris & Witter, 2009) to argue that Re is the critical structure for spatial memory.

The medial dorsal (MD) nuclei have important implications in working memory in rats and primates alike. Early work with non-human primates by Fuster and Alexander (1971) has demonstrated increased neuronal activity during the delay period of a memory task, both in mPFC and in the MD nuclei of thalamus which innervate it. Damage to MD nuclei in monkeys has also been found to impair spatial memory, although the delineation between impairments specific to processes intrinsic to thalamus and deficits resulting from severed communication with mPFC is not clear based on these results alone (Isseroff, Rosvold, Galkin & Goldman-Rakic, 1982). Bilateral inactivation of central thalamic nuclei including MD and neighboring intralaminar and midline nuclei using the $GABA_A$ agonist muscimol has been shown to impair DMTP performance and the localization of these effects are confirmed by anatomical control injections (Mair & Hembrook, 2008). Similar impairment has been produced by bilateral

infusions of lidocaine (Porter, Koch & Mair, 2001) and by discrete lesions with localized damage in the injection site (Burk & Mair, 1998; Bailey & Mair, 2005).

More recent recording studies by Wyder, Massoglia and Stanford (2003) have confirmed delay-related activity in central thalamus during performance of gaze-based memory tasks by monkeys. Many thalamic cells were found to be related directly to visual and motor responses, and certain cells even seemed to increase activity prior to delivery of reward, indicating a prediction or expectation of reinforcement presumably guided by memory of previous trials (Wyder, Massoglia & Stanford, 2003).

While there is currently little electrophysiological data on central thalamus function during memory delay periods, convergent evidence from lesion studies does show pronounced impairment on certain types of working memory task (Aggleton, Hunt, Nagle & Neave, 1996). However, the nature of dysfunction due to central thalamic damage tends to be distinct from the type of deficits seen with prefrontal damage (Mair, Burk & Porter, 1998). Actual delay-dependent impairments consistent with loss of working memory were only seen in rats with hippocampal lesions, with more generalized disruption seen with thalamic lesions. Damage to mPFC showed little impairment at all (Mair, Burk & Porter, 1998). These data indicate distinct functions for these regions, but cannot rule out meaningful connections among them. Knowing the importance of hippocampal formation to working spatial memory, and given the dense connections with mPFC via central thalamus, it is possible that discrete lesion studies may be missing some of the picture, and that thalamus's output to medial prefrontal regions may still be vital to its role in memory processing.

CHAPTER 3

Importance of Thalamocortical Communication

Recent evidence indicates that reciprocal connections between mPFC and central thalamic nuclei like MD may be performing secondary, or 'higher order' processing of information. Sherman and Guillery (2011) suggest transthalamic corticocortical circuits involving mPFC and MD serve a modulatory function as opposed to directly driving or being driven by a single population of cells. These pathways have been shown to depend at least in part on MD function to maintain connectivity and preserve cognitive function (Parnadeau et al., 2013). These data suggest the activity of mPFC neurons which follows direct sensory input but precedes direct motor output may be critically modulated by corticothalamocortical circuits which rely on central thalamic nuclei such as MD.

Additionally, changes observed in the coherence of local field potentials in thalamocortical circuits, representing synchronous activity of neuronal firing between these key regions, has been associated with cognitive function including working memory in human subjects (Sarnthein, Morel, Von Stein, & Jeanmonod, 2005). In other human studies, certain alterations in this type of coherence, characterized as thalamocortical dysrhythmia, have been found in patients with neurological disorders which impair their cognitive ability, including Parkinson's disease and depression (Llinás, Ribary, Jeanmonod, Kronberg, & Mitra, 1999). This suggests that not only is communication between thalamus and PFC involved in memory and planning, but that the way in which these areas coordinate neural activity is potentially implicated in disorders with far-reaching effects on cognition and even emotion regulation.

It is possible that the influence of thalamic input to medial prefrontal regions, and their impact on the function of reciprocal corticothalamocortical circuits, plays a major role in many of the higher order processing functions traditionally attributed to the prefrontal cortex alone, and that the roles both of these discrete regions play in memory, cognition ad executive function are more inextricably linked than once thought. A perspective which looks past localized individual roles in order to assess systems level changes across multiple brain regions which contribute to diverse cognitive and behavioral processes may be needed in order to more fully describe the underlying physiology of these intricate functions.

Connections between mPFC and central thalamus are unilateral, connecting the left hemisphere thalamus to the left mPFC only, without crossing the midline of the brain. Thus inactivating central thalamus in one hemisphere should affect mPFC functions in that hemisphere only, leaving the other hemisphere unaffected (Hoover & Vertes, 2007). Memory fucntions are largely performed separately in each hemisphere of the brain, such that major impairments typically only occur when activity is disrupted in both hemispheres simultaneously. As with many functions, a single hemisphere is usually capable of handling operations on its own when the other hemisphere is damaged or otherwise impaired.

The unilateral nature of primary thalamocortical connections, along with a growing amount of evidence for the distinct but related working memory functions of central thalamus and mPFC, provides a unique opportunity to directly study the nature of the afferent pathways connecting MD nuclei in central thalamus to corresponding mPFC in their respective hemispheres.

Research conducted in our lab indicates there are cells in PFC which alter activity in response to certain phases of the DNMTP task (Onos, Francoeur, Wormwood, Miller, Gibson &

Mair, manuscript in preparation). Some cells show a marked increase in activity during the delay period preceding a choice, while others seem to change the frequency of activity based on the directional movement of the animal. These data indicate that the cells in medial prefrontal cortex are encoding information related to the solution of memory-dependent tasks. Ongoing research in our lab (Mair, et al., 2015; Miller et al., 2014, November) has also identified similar cell types active in central thalamus, indicating the two areas may have certain properties in common, consistent with direct communication between them. This study builds on both of these projects to examine the influence of central thalamus on PFC memory function at a cellular level of analysis, with implications for a systems level understanding of the role of thalamocortical interactions in a wide range of neural and behavioral functions.

If indeed these regions are part of a functional memory circuit, one would expect manipulation of central thalamus within one hemisphere to produce changes in the activity of medial prefrontal cortical neurons, but only in the ipsilateral hemisphere, sparing the animal's ability to accurately perform tasks based on working memory and executive control while still allowing us to see how neurons typically associated with those same tasks change in the absence of thalamic innervation. In this way it would be possible to compare mPFC's function with and without thalamic input (and by association input from any other distributed systems which pass through central thalamus) in a single animal, in real time, as it performs a series of actions reliant on working memory and the ability to plan responses around learned rules and expected outcomes.

These findings indicate that neurons in central thalamus and mPFC both exhibit behaviorally linked patterns of activity, some of which represent memory traces over time, and

we suggest that the activity of mPFC neurons during the task will change significantly in the absence of thalamic input.

The goal of this research is to examine the influence of the central thalamus on the memory coding properties of neurons in PFC. We hypothesize that prefrontal memory function depends, in part, on inputs from central thalamus, and that cutting off this input will disrupt memory coding properties of PFC neurons. Specifically, cortical cells' ability to accurately represent task-relevant information is expected to manifest in targeted changes in firing rate found only in direct relation to critical events in the DNMTP task. If thalamus does, in fact, modulate the function of mPFC in order to more accurately predict outcomes and plan actions, the strength of this neural signal compared to background activity of the cell (i.e., activity between the critical task events) should decrease in the absence of thalamic input.

Here we recorded spike activity in mPFC neurons in a single hemisphere on a daily basis. When cells with readily identifiable waveforms were recorded, their defining features were noted so that individual cells can be tracked across three days of recording. The drivable tetrode array was kept in place for these three days, and inactivation of thalamus accomplished on day two using ipsilateral microinjections of the $GABA_A$ agonist muscimol. Day three consisted of recording mPFC activity after the drug has worn off to verify that the same cell can be found on each day and changes in its day two activity attributed to effects of central thalamic inactivation.

Animals were given unilateral microinjections of muscimol in central thalamus so that activity in ipsilateral mPFC (with intact thalamic input) before and after the inactivation day can be directly compared to activity on day two with pharmacologically inactivated thalamic input to assess cellular changes which may underlie past observations of memory impairment following bilateral thalamic inactivation (Mair & Hembrook, 2008).

METHODS

Subjects

8 male Long Evans (Blue Spruce) rats were obtained from Harlan Laboratories (Boston, MA) at approximately three weeks of age. Animals were housed in pairs for an additional week and allowed to acclimate to the animal vivarium before separation and were then handled daily. Housing consisted of clear polycarbonate tubs full of pine shavings with removable steel wire lids. Once subjects were implanted with indwelling recording arrays, the home tubs were suspended from steel shelves to allow more space overhead than was afforded by the wire lids. This was done in order to minimize any impact to the recording array and thus reduce potential damage or discomfort. The vivarium was maintained on a 12:12 h light: dark cycle with lights on at 07:00. All animals were allowed *ad libitum* access to food and water until they reached a weight of 200 grams, at which point they began a restricted watering schedule. Animals only received water as reinforcement during training and for a 30 minute period at the end of each day, close to the end of the 12 hour light cycle. All animals were monitored daily for health and care was provided by the Animal Resource Office. Animals were transported between the vivarium and the lab in their home tubs.

Apparatus

The operant chamber is octagonal and fabricated from clear polycarbonate with a painted wooden floor. Retractable levers are centered on four walls located in the corners of the box (N, E, S, W). Reinforcement (2 pulses equaling 0.1 ml tap water) is delivered through a plastic port located above each lever to by the activation of solenoid valves (LFAA1201518H, The Lee Co., Essex, CT). The top of the chamber is open to allow cables to be attached to record neural

activity from awake, behaving rats. The chamber is located in a Faraday cage to minimize electrical artifacts for recording. All wires are wrapped in copper tape and grounded to the cold water supply. A Dell computer located in a separate room is used to control the apparatus using MED-PC software (MED Associates, Georgia, VT). Droppings and urine are removed between sessions and the chamber is cleaned daily with Alconox residue free detergent and hot water. Full cleanings between each subject's session were deemed unnecessary as the same routes are traveled over and over again by all subjects, thus making potential odor traces useless to the animals in the solution of the task. A subject can be seen performing the task while being recorded in the operant chamber in Figure 1.

Behavioral Task

The dynamic delayed non-match to position (DNMTP) trials begin with one lever (randomly selected; for instance the N lever) extending. The start lever is retracted when pressed and the lever immediately to the right or left (randomly selected; E or W for this example) extends as the sample. The sample lever retracts after it is pressed, the start lever extends, and the 3 s delay period begins. After the delay period ends, a response on the start lever causes the choice levers to extend (to the immediate left or right of the start lever; E and W in this example). A correct non-match to sample response (W if E is the sample or vice versa) causes a light above the lever to turn on to signal the availability of reinforcement. Rats are run on two different versions of the program on alternating days, with the first version (E/W) always selecting either the E or W levers as the start levers, randomly choosing from these two options for each trial's first phase. On the following day animals would run on the N/S version in which the start levers are selected only from N and S, with the E and W levers serving as sample and choice (the task is diagrammed in Figure 2). Rats were required to perform at a 70% correct

criterion (completing all 60 trials) on the dynamic DNMTP program for at least three separate sessions, at which point they underwent surgery to implant single cannula tetrode recording arrays. Rats were allowed a one-week recovery period and then (barring any persistent injury or abnormal behavior) immediately began recording sessions. Rats ran once a day (typically 5 to 6 days a week) and had their electrode lowered by $1/8^{th}$ of a screw turn (.056 mm depth) on all three screws upon completion of at least 30 trials, or if they had not had their electrode lowered in the previous three days, so as to prevent gliosis from occluding the tetrode path. Once rats began performing at criterion accuracy, they were considered eligible for inactivation treatments.

Recording Equipment

Activity was recorded using an array of four tetrodes, each having four twisted 17.8 micron platinum iridium microwires (16 total), each attached to one pin in an 18 pin Mill-Max (Mill-Max mfg. Corp., Oyster Bay, NY) plug. These tetrode bundles are threaded through a single stainless steel cannula and secured in place with epoxy at the point where they enter the cannula. This cannula is attached to one of the two central pins in the plug. The pin adjacent to the cannula is attached to a silver reference wire to be implanted alongside the recording cannula in the opposite hemisphere to provide a measure of baseline cortical activity against which to compare changes recorded by the tetrode array (the implant structure can be seen in Figure 3).

The array containing the tetrodes, cannula and Mill-Max plug was embedded in dental acrylic (Dentsply, York, PA) and attached to three custom cut machine screws (the finished implant can be seen attached to a subject in Figure 4). These screws were fitted into threaded nylon bases which allowed them to be lowered into the bases at set intervals so that the entire

tetrode array can be steadily advanced through PL and IL moving from dorsal to ventral regions of the target area.

Prior to implantation, electrodes were tested with the Nano-Z (Neuralynx, Bozeman, MT) and plated with platinum black to lower impedances to a target of ≤ 200 mega ohms. Once implanted, a cable extending from low torque slip-ring commutator (Dragonfly Research and Development, Inc., Ridgeley, WV) was attached to the electrode and signals were sent through to the Neuralynx Digital Lynx SX system in an adjoining room. Recorded raw signals were amplified and sent through the Neuralynx Digital Lynx SX to be processed using the Cheetah data acquisition software. Digital signal processing (DSP) low cut and high cut filters were set at 600 to 6,000 Hz. DSP employs a Finite Impulse Response (FIR) filter, and the resulting signal was displayed as the Continuously Sampled Channel (CSC). The FIR was used only for frequencies from 150 to 9,000 Hz in the input range. A digital controlled oscillator (DCO) filter is used for frequencies between 0.1 Hz and 150 Hz and used a running average to remove the direct current component from the alternating current signal. The Cheetah acquisition software automatically selects the filter type depending on the range input by the user when filtering turned on. Spike detection is set to threshold with retrigger set at 750 μs. The input range typically varied between 200 to 400 μv and spike thresholds were changed daily based upon the strength of the signal. During inactivation sequences, thresholds were maintained across all three days at the levels set on the pre-inactivation day in order to record cellular activity using consistent parameters. A super port (DIG-726-TTL card) connected to the interface (Med Associates) sent TTL pulses to the Neuralynx Digital Lynx SX. These TTL pulses generated a specific time stamp in relation to key stages in the task (e.g: lever pressing responses during the start, sample or choice phase of the trial or the delivery of water reinforcement) and enable the

correlation of the flagged behavioral event to specific neural responses. A Neuralynx video tracking system was also used to keep a moment-to-moment record of where the rat was located and the direction of its head and movement within the apparatus by tracking two LEDs affixed to the plug that attaches the electrode.

Surgical Procedure

All surgical instruments were sterilized prior to surgery in an autoclave or, if the tools will not fit in the autoclave, by submersion overnight in 70% ethanol. Rats were anesthetized using a combination of Ketamine (80 mg per kg body weight) and Xylazine (8 mg per kg body weight), injected using a 1 ml syringe with a 25 gauge stainless steel needle. Once deep anesthesia was achieved, any hair in the surgical field was shaved off and ointment was applied to the eyes to prevent drying. At this point the rat's head was secured by the earbars of the angled stereotaxic instrument (Stoelting, Wood Dale, IL) and the skin in the area of the incision was cleaned with Betadine (a povidone iodine solution). A longitudinal incision was made along the midline of the skull, the skin was retracted to expose the surgical field, and the periosteum was scraped away. The stereotaxic plane was verified by measuring the locations of Bregma and Lambda sutures on the surface of the skull relative to the interaural line.

The skull was then opened with a burr bit to expose the dorsal surface of the brain. Stereotaxic coordinates for the tetrode placement were measured in mm relative to Bregma for AP and relative to surface of cortex for DV. The skull above the electrode target, +3.0 AP, is opened to allow space for a cannula to enter one hemisphere 0.5 mm off midline, and the electrical reference wire to enter the opposite hemisphere 0.5 mm off midline such that both should pass through the entirety of PL and IL as the cannulae are lowered. The burr bit was then

used to expose the dorsal surface of the brain above the injection target site, 5.0 mm off the sagittal suture at -2.8 AP.

All supplies for implanting cannulae (guide cannulae, internal cannulae, dummy cannulae, dust caps, tubing and adapters, and stainless steel machine screws) were obtained from Plastics One (Roanoke, VA). Cannulae were custom sized for making infusions into MD. Cannulae and machine screws were sterilized using the same procedures used for surgical instruments. Four small holes were drilled in the skull around each of the implantation sites (8 holes in all) so that stainless steel machine screws could be inserted in order to hold the implants in place. Screws were placed so that they did not reach through the skull to the dura mater and their tops extended above the skull.

The injection guide cannula tip was positioned at approximately -3.2 DV, -2.8 AP, with coordinates relative to Bregma for AP and DV. The cannula was lowered into place at an angle so that the exposed end was not obstructed by the feet of the electrode array. It was placed such that when a 28 gauge internal cannula extending 2.0 mm beyond the end of the guide is inserted for injections it will be at -5.2 DV, -2.8 AP, just outside the center of the MD nucleus in central thalamus. Once the cannula was lowered into place, it was secured to the surrounding skull screws using grip cement (Dentsply, York, PA) and allowed to set for 10 minutes.

At this point, surface of cortex at the tetrodes implant site was visually confirmed by touching the tetrodes to the dura mater, at which point the recording array is pulled up to allow the meninges in the area to be removed with a recurved needle, at which point the tetrodes were returned to cortex surface and lowered 1.0 mm below it. Once the tetrode cannulae are in place, the three feet into which the machine screws were threaded are fixed to the skull screws using

grip cement, which was then built up around the implant to secure the base to the skull and prevent access to the implant site, which is surrounded in sterile Vaseline to maintain a sterile barrier and allow the cannulae to be driven smoothly through cortex. The surgical dummy cannula was removed from the guide cannula and replaced with a dummy cannula with a threaded dust cap which was then secured over the top of the guide.

The inner sides of the incision immediately anterior and posterior to the implant area were then carefully opposed and the incision closed with sterile silk sutures. The suture line was irrigated with Betadine and the rat was transferred to a clean polycarbonate tub where it was kept warm and monitored until it recovered from the effects of the anesthesia. Rats were administered Butorphanol via SC injection using a 1 ml syringe with a 25 gauge stainless steel needle following surgery. This was done to alleviate irritation caused by surgery, particularly from the implanted cannulae, and speed recovery from surgery.

Microinjection Procedure

Before microinjections were administered, each animal was required to meet performance criteria the task following recovery, again achieving an average correct choice percentage of 70% or higher for 3 sessions. Rats were wrapped in a towel and hand held during the microinjection procedure. Treatments were administered via a 28 gauge internal cannula (Plastics One, Roanoke, VA) attached to a 250-µL syringe (Hamilton, Reno, NV) driven by a minipump (Harvard Apparatus, Holliston, MA). All equipment were sterilized with 70% ethanol before the drug is drawn up into the tubing. The internal cannula extends approximately 2 mm below the tip of the implanted guide cannula. All injections of muscimol consisted of of 0.25-µL volume and were delivered at a rate of 1.0-µL/min. Injections will consisted of either 0.25, 0.5,

1.0, or 2.0 nmol total muscimol. The internal cannula was left in place for an additional 60 seconds after injection to ensure diffusion of the drug. Animals were then returned to their home cage to rest for 10 minutes while the drug took effect, after which they were transported to the operant chamber to begin the task. Injections were repeated if any equipment malfunctions occurred during the microinjection procedure prior to drug delivery.

Histological Analysis

At the completion of behavioral testing, the ends of the tetrode tracks were marked by creating electrolytic lesions, where 50 μA of current was passed for 30 seconds through the tetrode bundle that yielded the highest number of cells, and waiting 3 days before sacrificing the animals for gliosis to develop around the site. This produces a visible lesion marking the end of the tetrodes from which the depth of the implant at each recording session can be inferred based on the documented increments at which it was lowered. All animals were sacrificed under deep anesthesia (100 mg/kg ketamine, 10 mg/kg xylazine) by transcardiac perfusion of 0.9% physiological saline followed by 4% (v/v) neutral buffered formalin. Electrodes were slowly and completely backed out using the machine screws to minimize post-mortem damage to the site.

Brains were extracted from the skull and immersed in 10% formalin, 10% DMSO, and 30% sucrose in neutral phosphate buffer for a minimum of 24 hours. Tissue was then sectioned frozen in the coronal plane at 50 μm and stained with thionin to confirm electrode placement and path as well as injection cannula placement. Tissue was also examined for any other signs of infection or damage.

Data Analysis

Data consisted of continuous digital records throughout 60-minute behavioral sessions along with activity from each of the 16 microwires, TTL pulses marking behavioral events with specific time stamps, and HD video tracking records. Analyses of microwire recordings utilize SpikeSort3D software to identify action potentials originating from discrete neurons.

KlustaKwik is a tool used in SpikeSort3D (Neuralynx) that allows the assessment of waveform patterns based upon a variety of measures such as changes in amplitude such as change between peak and trough, distance from peak to valley as well as distance from valley to valley. This is used to automatically cluster waveforms that are determined to have similar attributes in 3D space based upon peak comparisons. Upon examination of these waveforms, a number of criteria were used to assess whether the waveform was indeed cellular activity or indicative of electrical noise. In order for a waveform to pass this first stage of analysis and be assessed in relation to the task, waveforms must demonstrate the following: (a) a clear difference in peak size and/or shape across the four tetrode windows (one for each recording microwire) (b) form a distinct cluster in the 3D plot (c) show an acceptable inter-spike interval histogram displaying a normal peak with a high frequency of spike pairs falling in the optimal range of 10 to 10,000 milliseconds (d) a signal to noise ratio (ratio of peak amplitude to the maximum amplitude recorded in the waveform's tail following repolarization) of at least 1.5:1 (e) the hyperpolarization should be smaller than the depolarization, and not symmetric to it. These criteria were also used to track single cells throughout the three day inactivation sequence, with waveform shape, ISI distribution, and cluster shape and location being analyzed for similarities across all days to verify each cell's identity (See Figure 5). Only when cells with distinct and recognizable waveforms and clusters were found on a recording day would the

subject be scheduled for thalamic inactivation on the following day, increasing the chances that we could identify the same cell over the next two days of recording.

Once waveforms were identified as meeting these criteria, their activity and correlation to specific stages of the behavioral task are assessed using NeuroExplorer software (Neuralynx). NeuroExplorer calculated the average firing rate (in spikes per second) of every identified cell across the entire session, which allowed us to compare the general level of activity of any given cell before, during, and after thalamic inactivation.

In order to assess changes in activity related to discrete phases of the DNMTP task, raster-plots and peri-event time histograms (PETHs) were generated for all identified waveforms. Raster-plots show frequency of firing of a particular neuron over the course of a trial for all trials recorded and examination of these plots enables the confirmation of consistent activity (whether this is firing or absence of firing) throughout the entire behavioral session and surrounding the event marker (raster plot and PETH can be seen in Figure 6). PETHs are generated to demonstrate a change in activity of a neuron that is related to a specific event or location by averaging its activity when a common event or location is repeated across the behavioral session. All PETHs plot the firing rate of a cell (in spikes per second) five seconds prior to and five seconds after an event marker, organizing the activity into 50 bins which each contained 200 msec.

A second set of PETHs were then made which show the cell's activity as well as a visual representation of the average firing rate of that cell during the entire session. This average activity is shown on the plot as a dotted line within a band representing a 99% confidence interval, such that any activity on the histogram which falls below the band is significantly lower

than average firing, and any activity above it is significantly higher than the average level (See Figure 7). In this way cells can be identified not only as showing increases or decreases in firing rate surrounding key events, but these changes can be evaluated for significance.

Peak Signal-to-Noise

During the three-day sequences when a subject received a thalamic inactivation injection, further analyses were performed using the PETHs with illustrated confidence intervals. Peak activity during each of the event-related windows was calculated as the firing rate within the single highest bin in the ten second window, this firing rate was then transformed into a Z-score relative to the background firing rate of the cell within the 10 second event window. Background firing rate was calculated as the mean firing rate inside each event window, excluding the bins within one second of the peak bin on either side in order to avoid counting activity in the shoulders of each peak as part of the background cell activity.

Z-scores were calculated by subtracting background mean firing rate from peak firing rate, and dividing the result by the standard deviation of the background mean rate. In this way, the key changes in firing which centered around specific events and allowed us to identify cells as being related to certain behavioral events could be quantified relative to the cell's background, or uncorrelated, activity. These peak Z-scores allowed us to numerically represent the approximate maximal signal-to-noise ratio of a cell's peak signal-to-noise relative to each event in the task.

We then selected the window which best captured the critical event-related changes for each cell type. Movement related cells were characterized by their response immediately before and after lever presses, so the end-of-delay lever press was chosen as a representative sample as

it captured a moment in the middle of the DNMTP task when the animal would be traveling between sample and choice levers. This avoided reinforcement related changes as well as the inter-trial interval seen preceding the start lever.

Base lever cells were characterized by their sharp increases in activity at the base levers in the task, when trials were started and delay period were ended in order to initiate the choice phase. For this reason, the end-of-delay lever press window was also used to measure the magnitude of action cells' response, again avoiding changes in activity during the inter-trial interval which may have skewed firing rates around the start lever presses.

The rest of the cell types recorded during inactivation sequences were all characterized by their activity surrounding the delivery of reinforcement during the task. These were: reinforcement anticipation cells, which increased activity leading up to the first delivery of water reinforcement and remained active through the second pulse of water; reinforcement excitation cells, which began a sharp increase in activity just after the first pulse of water and declined after the second pulse; and finally post reinforcement cells, which showed a large increase in firing rate beginning just after the second pulse of water was delivered and tended to remain highly active for seconds afterward.

All three of these cells were identified by their relation to reinforcement delivery, and were measured by peak Z-scores within the reinforcement PETH window. In this way we were able not only to identify significant increases in firing rate tied to specific events, but also to quantify the signal-to-noise ratio of these behaviorally correlated changes in cell activity as compared to the background activity of the cell within the event-related windows which best represented the typical behavior of each cell type. These peak Z-scores allowed us to compare

the specificity of each cell's action across multiple cell types and subjects using a standard metric, and to evaluate the effect of thalamic inactivation on the signal-to-noise properties which illustrate the degree of clarity with which the cell responds to critical events in the task which likely relate to the encoding and planning of key actions and outcomes. PETH windows around the end-of-delay lever press from a base lever cell can be seen in Figure 8 on pre-inactivation, inactivation, and post-inactivation days.

Average Signal-to-Noise

This measure provided a consistent estimate of signal-to-noise properties driven by the cell's activity at its peak rate of firing, compared to a relatively narrow background surrounding the relevant event. In order to characterize broader patterns of signal-to-noise features across cell types, a second set of analyses was conducted using a measure of average signal-to-noise which incorporated data from the entire recording session in order to measure total mean firing activity within a set window of time around a given event (or events) by which cell types were initially classified.

These time windows were defined by previous work in categorizing cell types based on timing of activity changes, and correspond to the average periods during which activity was significantly higher than background mean firing (as assessed in the probability PETH).

Movement cells were defined by increased firing between 1.3s before the start lever press and 0.5s before the start lever press; 0.5s after the start lever press to 1.5s after the press; 0.9s before end-of-delay lever press to 0.4s before delay lever press, and 0.5s after the delay lever press to 1.3s after the press. These four periods of activity made up the defining peaks of movement cell firing. Thus, the mean firing rate was calculated within these time windows

across all trials in the session, and these rates were averaged together to provide a single target mean firing rate for movement cells.

Base lever cells were defined by peak activity during base lever presses, specifically from 0.7s before the start lever press to 0.3s after the press, and from 0,6s before the end-of-delay lever press until 0.2s after it.

Reinforcement excitation cells showed peak activity between 0.2s after the first pulse of water delivered and 2.3s after this pulse (1.3s after the second and final water pulse).

Reinforcement anticipation cells were most active between 1.0s before the first pulse of water and 1.5s after (0.5s after the second water pulse).

Post-reinforcement cells were most active between 2.0s after the first water pulse (1.0s after the second) and 3.5s after the first pulse (2.5s after the second).

Once target mean firing rate was calculated within the given windows for each type of cell, background mean firing was calculated by subtracting the total time accounted for within the target window (across all trials in the session) from the total time the animal ran the task; then subtracting the total number of spikes recorded within the target window from the total number of spikes recorded from the cell over the entire session. By dividing the total spike count outside the target window by the total time outside the target window, we calculated the mean firing rate of the cell during the entirety of the recording session which was not included in the target window. Target mean firing rate was then divided by background mean firing rate to provide a measure of average signal-to-noise which incorporated all of the cell's recorded activity as opposed to a single event-related window. All firing rate and spike count calculations were performed in NeuroExplorer.

PETH Pattern Correlation

In order to assess the similarity in the general shape, or pattern of cell activity surrounding key events, we conducted a correlation analyses of the PETH data for the relevant 10s windows around each cell type's critical task events. Each window is made up of 50 200ms bins, each with its own firing rate. By correlating firing rate in each bin on pre-inactivation days with the identical bin firing rate on inactivation and post-inactivation days, we were able to numerically represent the consistency of the PETH shape across the inactivation protocol in terms of Pearson product-moment correlation coefficients (Pearson's *r*). For cells which showed clear patterns in multiple windows (e.g., movement and base lever cells during start lever and delay lever presses) the *r* values for both widows were averaged together. This analyses assessed moment-to-moment changes in cell activity before, during and after the critical event, and allowed us to objectively compare the observed pattern of firing rate over time as it changed during and after thalamic inactivation.

Place Map Pattern Correlation

Finally, in order to assess changes in the pattern of location-specific cell activity we conducted correlation analyses of video tracking data. Place field analyses were conducted using NeuroExplorer to measure the rate of cell firing in a 70 by 70 grid of bins covering the behavioral arena with a minimal time/bin of 0.2s and minimum of 3 visits in the recording session. These data were used to create heat maps showing spatial areas with the highest rates of firing (See Figure 9). A subset of neurons had spatial heat maps that revealed areas of activation restricted to 50% or less of the broader area associated with a behavioral event, these cells were determined to be related to spatial context (the same method used in Onos, et al., manuscript in preparation).

Numeric data from the heat maps was used to correlate activity in each of the bins on pre-inactivation days with the corresponding bins on inactivation and post-inactivation days. In this way the consistency among heat maps could be objectively compared across all three days of the inactivation protocol. Similar analyses have been used to confirm consistency across comparable sessions in place field data (Rowland, Yanovich, & Kentros, 2011). Again, Pearson's *r* was used to represent the strength of correlation between spatial heat maps. This analyses allowed us to objectively quantify the pattern of cell activity as it related to the animal's location in the recording chamber, and to measure changes in this pattern during inactivation by comparing the strength of correlation between pre- and post-inactivation days to the strength of correlation between pre-inactivation and inactivation days. We were also able to independently assess changes in pattern within those cells which seemed to exhibit context-dependent activity on pre-inactivation days.

Statistical Analyses

Once these data were collected and processed in NeuroExplorer, statistical analyses were conducted in SPSS (IBM) in order to test whether thalamic inactivation produced significant alterations in the overall cell activity (mean firing rate), peak signal-to-noise (peak Z-scores), average signal-to-noise, correlation strength between PETHs, correlation strength between place maps, and accuracy of DNMTP task performance (proportion of correct responses over the entire session). Based on the hypothesis that central thalamic input to PFC serves to sharpen the coding properties of cortical neurons via modulatory pathways, we predicted that inactivation would produce a decrease in signal-to-noise properties of cortical neurons, represented by a negative change in peak Z-scores, as well as average signal-to noise scores, relative to both pre- and post-inactivation days.

Given the hypothesis that cells should return to their normal level and pattern of activity the day after thalamic inactivation, we also predicted that correlations between PETH data should be significantly stronger between pre- and post-inactivation days as compared to the correlation between pre-inactivation and inactivation days. This would support the hypothesis that the overall pattern of event-related activity, as well as more targeted measures of signal-to-noise properties, would shift during thalamic inactivation.

As not all cells initially exhibited location-specific firing on the first day of recording, we had no specific hypothesis as to the correlation between place maps across days. However, we did predict that those cells which did show signs of location-specific firing should be more strongly related on pre- and post-inactivation days as compared to pre-inactivation and inactivation days.

Given the density of both inhibitory and excitatory interneurons in medial PFC, we did not necessarily expect a significant change in mean firing rate in either direction, as cutting off excitatory input from central thalamus could indirectly produce both inhibition and disinhibition in the recorded cells. For this reason we also considered the direction of change in activity (i.e., whether the cell's mean firing rate increased or decreased during inactivation days) as a potential moderating variable in order to assess any differences in results for these two response types.

Finally, as the unilateral manipulation should effectively spare an intact hemisphere and all related thalamocortical function involved in successful completion of the DNMTP task, we predicted that the proportion of correct responses would not change significantly across all three days of the inactivation sequence.

RESULTS

Histological Results

Histological assessment of the sectioned, thionin-stained brain tissue from the five rats included in the final data analysis revealed the exact placement of injection cannulae and the tracks along which recording tetrodes were lowered. Exact coordinates for injection cannulae can be found in Table 1, and coordinates marking the endpoint lesions made by recording tetrodes can be seen in Table 2. A diagram of the approximate injection sites can be seen in Figure 10, tracks of the recording tetrode cannulae are shown in Figures 11 through 15, with the approximate position of the array at each analyzed inactivation day marked with numbered hash marks.

These findings indicate that all recording arrays were placed within the target regions, although several began recording in areas closer to AC than PL and IL. Inactivation cannulae were all in the vicinity of MD, but two subjects had cannulae terminating in a location dorsal to the target, and two had cannulae terminating in areas lateral to the target. For this reason, location of injection cannula was treated as a potential moderator in further analyses, with subjects identified as having Dorsal, Lateral, or On Target cannula locations.

Results of Data Analyses

Of the eight rats initially trained and implanted with recording units for the experiment, five are included in the following analyses. These five subjects were the only rats from which cells were recorded, identified, and accurately tracked across at least one three day inactivation

sequence. The excluded subjects exhibited no cell recordings which could be verified across all three days, and thus provided no usable inactivation data.

Overall Analyses (44 unique cells across 5 rats and 28 "days")

Task Performance. Contrary to predictions, a one-way repeated measures ANOVA revealed a significant effect of day (pre-inactivation, inactivation, post-inactivation) on the proportion of correct responses, $F(2,54)=7.23$, $p<.05$ (See Figure 16). A post-hoc LSD test revealed that the proportion of correct responses was significantly lower on inactivation days ($M=0.74$, $SD=0.08$) compared to on pre-inactivation days ($M=0.79$, $SD=0.08$) and post-inactivation days ($M=0.80$, $SD=0.07$), $ps<.05$. The post-hoc comparisons also revealed that the proportion of correct responses did not significantly differ on pre-inactivation and post-inactivation days, $p>.05$. This pattern suggests that muscimol injections significantly impaired performance on injection days.

Mean Firing Rate. A one-way repeated measures ANOVA revealed a significant effect of day on mean firing rate, $F(2,86)=4.49$, $p<.05$ (See Figure 17). A post-hoc LSD test revealed that across all cells mean firing rate was significantly higher on pre-inactivation days ($M=7.80$, $SD=6.23$) than on inactivation days ($M=4.90$, $SD=4.70$), $p<.05$. Mean firing rate on post-inactivation days ($M=5.92$, $SD=5.48$) did not differ significantly from mean firing rate on either pre-inactivation or inactivation days, $ps>.05$. Thus, mean firing rate appears to have only partially recovered to pre-inactivation day levels on post-inactivation days.

Peak signal-to-noise. We conducted a planned quadratic contrast to specifically test whether the pattern of peak signal-to-noise (i.e., peak Z-scores for type-relevant PETH window) across days fit our predictions (i.e., less peak signal-to-noise on inactivation days compared to

both pre- and post-inactivation days). The quadratic contrast failed to reach significance, $F(1,43)=1.15$, $p>.05$, indicating that changes in peak signal-to-noise across days did not fit the predicted pattern. We then conducted a one-way repeated measures ANOVA to examine whether there were any differences in peak signal-to-noise across days. This analysis revealed only a marginally significant effect of day on peak signal-to-noise, $F(2,86)=2.29$, $p=.11$ (See Figure 18). A post-hoc LSD test revealed that peak signal-to-noise was marginally higher on pre-inactivation days ($M=5.86$, $SD=3.30$) than on both inactivation days ($M=5.01$, $SD=2.79$) and post-inactivation days ($M=4.99$, $SD=3.20$), $ps<.08$, and that peak signal-to-noise did not significantly differ on inactivation and post-inactivation days, $p>.05$.

Targeted Analyses Excluding Later Injection Data

The results of the initial analyses did not fit the predicted pattern, revealing less recovery than expected of peak signal-to-noise on post-inactivation days, as well as impaired task performance on inactivation days. The fact that behavior was impaired by the drug suggests collateral effects which should not be associated with unilateral manipulations, and raised questions about detrimental effects produced by repeated intracerebral injections.

Two of the included subjects continued running inactivation trials well past the others, receiving considerably more intracerebral infusions of muscimol, and risking more long term damage than the other subjects. In order to maintain consistency across results from all subjects, only the first six inactivation sequences were included in the final analyses. This was done due to concerns that such a large number of infusions could be altering the thalamic tissue in unpredictable ways, a concern borne out by increased difficulty in identifying cells across all

three days due to unpredictable changes in the clusters and firing rates which were not seen in the earlier inactivation sequences.

Long term effects of muscimol infusions of the kind used in this experiment are not well described, but there is evidence that repeated activation of $GABA_A$ receptors has been associated with cell death in developing cells (Honegger, Pardo & Monnet-Tschudi, 1998; Xu et al., 2000) and other research has cautioned against potential ill effects of chronic intracerebral injections of muscimol and other $GABA_A$ agonists (Lomber, 1999; Malpeli, 1999). This, coupled with the risks of mechanical damage from repeated infusions and the erratic recording results, lead us to consider only earlier inactivation sequences when conducting final statistical analyses. Evidence of damage was in fact observed, demonstrated by the appearance of hemosiderin deposits - associated with the tissue's response to trauma (Iancu, 1992) - surrounding the injection site, but only in the subject that received the highest number of injections (see Figure 19), lending support to the concerns regarding additive effects of repeated injections.

We took the median number of inactivations across all rats, six, and decided to exclude any data from inactivation sequences exceeding this median in order to compare all subjects on more equal footing, and ignore cellular activity likely to be associated with unexpected collateral impairment of behavior. The analyses of the refined data follow (Analyses comparing the data collected from the first 6 inactivation protocols to those collected from later sessions can be found in Appendix D).

Targeted Analyses (Only the first 6 inactivations; 21 unique cells across 5 rats and 15 "days")

Task Performance. As predicted, and contrary to the results calculated using all inactivation protocols, a one-way repeated measures ANOVA failed to reveal a significant effect

of day (pre-inactivation, inactivation, post-inactivation) on the proportion of correct responses, $F(2, 28)=3.01$, $p>.05$ (See Figure 20). Thus, for the first 6 inactivation protocols, muscimol injections did not produce significant decrements in task performance on injection days.

Mean Firing Rate. A one-way repeated measures ANOVA revealed a significant effect of day on mean firing rate, $F(2,40)=6.85$, $p<.05$ (See Figure 21). A post-hoc LSD test revealed that across all cells mean firing rate was significantly higher on pre-inactivation days ($M=9.73$, $SD=7.26$) than on both inactivation days ($M=4.49$, $SD=4.34$) and post-inactivation days ($M=5.07$, $SD=5.37$), ps$<.05$, and that mean firing rate did not significantly differ on inactivation and post-inactivation days, $p>.05$. Thus, consistent with the results calculated using all inactivation protocols, analyses on the first 6 inactivation protocols revealed that mean firing rate decreased on inactivation days and failed to recover to pre-inactivation day levels on post-inactivation days.

Potential Moderators of Mean Firing Rate

To test for potential moderators of the observed pattern in mean firing rate across days, we conducted a series of mixed-model ANOVAs with day as the repeated measure, each moderator as a between-subject variable, and mean firing rate as the dependent variable. Moderating variables included dose of muscimol injection (i.e., low (.25 nmol or .5 nmol), medium (1 nmol), high (2 nmol)), location of the injection site (i.e., lateral to target, dorsal to target, on target), cell type (i.e., base lever cells, movement cells, reinforcement excitation cells, reinforcement anticipation cells, and post-reinforcement cells), and direction of mean firing rate change (i.e., increase vs. decrease in mean firing rate from pre-inactivation day to inactivation day). As the lowest muscimol dose (.25 nmol) was only used once in a single subject, the low

dose condition collapsed findings across this and the .5 nmol level, considering them comparable.

Injection Location. The mixed-model ANOVA with day as a repeated measure and injection location as a between-subjects factor revealed only a marginally significant main effect of location on mean firing rate, $F(2,18)=2.10$, $p=.15$. A post-hoc LSD test revealed that overall mean firing rate was marginally lower for lateral injection locations ($M=9.97$, $SD=3.86$) compared to dorsal ($M=5.40$, $SD=3.86$) and on-target ($M=5.88$, $SD=3.86$) locations, ps$<.11$. Mean firing rate for dorsal and on-target injection locations did not differ significantly, $p>.05$. The mixed-model ANOVA also revealed a significant interaction between day and location on mean firing rate, $F(4,36)=3.89$, $p<.05$. To further investigate this interaction, we conducted a series of repeated-measures ANOVAs to evaluate the effect of day on mean firing rate separately within each injection location group. These analyses revealed that the effect of day on mean firing rate only reached significance for cells with on-target injection locations, $F(2,12)=8.20$, $p<.05$. A post-hoc LSD test revealed that for cells with on-target injection locations, mean firing rate was significantly higher on pre-inactivation days ($M=13.23$, $SD=9.87$) compared to both inactivation ($M=0.87$, $SD=0.53$) and post-inactivation days ($M=3.54$, $SD=5.16$), $p<.05$. Inactivation and post-inactivation mean firing rates did not differ significantly for cells with on-target injection locations, $p>.05$. The repeated-measures ANOVA for cells with dorsal injection locations revealed only a marginally significant effect of day on mean firing rate, $F(2,18)=3.38$, $p=.06$. A post-hoc LSD test revealed that, for cells with dorsal injection locations, mean firing rate was significantly higher on pre-inactivation days ($M=7.16$, $SD=5.34$) than on post-inactivation days ($M=3.88$, $SD=2.12$), $p<.05$. Mean firing rate on inactivation days ($M=5.18$, $SD=3.13$) did not differ significantly from either pre- or post-inactivation days for cells with

dorsal injection locations, *ps*>.05. The repeated-measures ANOVA failed to reveal a significant effect of day on mean firing rate for cells with lateral injection sites, $F<1$.

Dose. The mixed-model ANOVA with day as a repeated measure and dose condition as a between-subject factor revealed a significant main effect of dose on mean firing rate, $F(2,18)=4.48$, $p<.05$. A post-hoc LSD test revealed that overall mean firing rate was significantly higher in the low dose condition ($M=9.52$, $SD=3.52$) compared to the medium dose condition ($M=4.44$, $SD=3.52$) Mean firing rate in the high dose condition ($M=6.52$, $SD=3.52$) did not differ significantly from either low or medium dose conditions, *p*s>.05. The mixed-model ANOVA failed to reveal a significant interaction between day and dose on mean firing rate, $F(4,36)=2.00$, $p>.05$.

Cell Type. The mixed-model ANOVA with day as a repeated measure and cell type as a between-subject factor failed to reveal a significant main effect of cell type on mean firing rate, $F(4,16)=1.47$, $p>.05$. It also failed to reveal any significant interaction between day and cell type on mean firing rate, $F(8,32)=1.38$, $p>.05$.

Direction of Change. The mixed-model ANOVA with day as a repeated measure and direction of change as a between-subject factor failed to reveal a significant main effect of direction on mean firing rate, $F<1$. Predictably, the mixed-model ANOVA did reveal a significant interaction between day and direction of change on mean firing rate, $F(2,38)=6.80$, $p<.05$. To further investigate this interaction, we conducted a series of repeated-measures ANOVAs to evaluate the effect of day on mean firing rate separately within cells which increased activity during inactivation and those which decreased activity during inactivation. These analyses revealed that the effect of day on mean firing rate only reached significance for

cells which decreased activity on inactivation days, $F(2,28)=12.39$, $p<.05$. A post-hoc LSD test revealed that for cells showing decreased activity, mean firing rate was significantly higher on pre-inactivation days ($M=11.55$, $SD=7.58$) compared to both inactivation ($M=3.28$, $SD=3.10$) and post-inactivation days ($M=4.50$, $SD=4.34$), $p<.05$. Inactivation and post-inactivation mean firing rates did not differ significantly for cells showing decreased activity during inactivation, $p>.05$. The repeated-measures ANOVA for cells with increased activity during inactivation failed to reveal a significant effect of day on mean firing rate, $F(2,10)=1.14$, $p>.05$. It is worth noting that of the 21 cells included in the analyses, only 6 showed increased mean firing rate during inactivation, and thus our ability to accurately assess effects within this restricted sample was limited by the small *n*.

Peak Signal-to-Noise. We conducted a planned quadratic contrast to specifically test whether the pattern of peak signal-to-noise across days fit our predictions (i.e., lower peak Z-scores on inactivation days compared to both pre- and post-inactivation days). As predicted, and contrary to the results calculated using all inactivation protocols, the quadratic contrast for the first 6 inactivation protocols was significant, $F(1,20)=7.71$ $p<.05$. The residual for the quadratic contrast was not significant, $F<1$, indicating that the quadratic successfully explained the pattern of peak signal-to-noise across days (See Figure 22). Thus, for the first 6 inactivation protocols, peak signal-to-noise was significantly reduced on inactivation days compared to both pre- and post-inactivation days.

Potential Moderators of Peak signal-to-noise.

Injection Location. The mixed-model ANOVA with day as a repeated measure and injection location as a between-subject factor revealed no significant main effect of location on

peak signal-to-noise, $F<1$. It also failed to reveal any significant interactions between day and location of injection on peak signal-to-noise, $F(4,36)=1.05$, $p>.05$.

Dose. The mixed-model ANOVA with day as a repeated measure and dose as a between-subject factor failed to reveal a significant main effect of location on peak signal-to-noise, $F(2,18)=1.44$, $p>.05$. It also failed to reveal any significant interaction between day and dose on peak signal-to-noise, $F(4,36)=2.09$, $p>.05$.

Cell Type. The mixed-model ANOVA with day as a repeated measure and cell type as a between-subject factor revealed a significant main effect of cell type on peak signal-to-noise, $F(4,16)=4.39$, $p<.05$. A post-hoc LSD test revealed that for base lever cells, overall peak signal-to-noise was significantly higher compared to post-reinforcement, reinforcement-anticipation, and reinforcement excitation cells (ps$<.05$), and marginally higher compared to motion cells, $p=.08$. Moreover, for post-reinforcement cells, peak signal-to-noise was significantly lower compared to base lever and motion cells (ps$<.05$), and marginally lower compared to reinforcement-anticipation and reinforcement-excitation cells, ps$<.12$. All other comparisons failed to reach significance, ps$>.05$ (see Figure 23 for means and standard errors). The mixed-model ANOVA failed to reveal any significant interaction between day and cell type on peak signal-to-noise, $F(8,32)=1.05$, $p>.05$. While this interaction effect failed to reach significance, visual inspection of Figure 23 suggests that analyses may have merely been underpowered to detect an interaction between cell type and day on peak signal-to-noise; the predicted quadratic pattern (i.e., less peak signal-to-noise on inactivation days compared to pre- and post-inactivation days) is noticeably more pronounced in base lever cells compared to all other cell types.

Direction of Change. The mixed-model ANOVA with day as a repeated measure and direction of change as a between-subject factor revealed only a marginally significant main effect of direction of change on event specific activity, $F(1,19)=3.44$, $p=.08$, such that event specific activity overall was greater in cells which showed decreased mean firing rate during inactivation ($M=5.97$, $SD=2.25$) compared to those which showed increased mean firing rate during inactivation ($M=3.95$, $SD=2.25$). The mixed-model ANOVA failed to reveal any significant interaction between day and direction of change on peak signal-to-noise, $F<1$.

Average Signal-to Noise. A repeated-measures ANOVA failed to reveal any significant effect of inactivation day on average signal-to-noise, $F<1$. However, the means trended in the predicted direction, such that average signal-to-noise was lowest on inactivation days ($M=1.54$, $SD=1.16$), compared to both pre-inactivation days ($M=1.80$, $SD=1.13$) and post-inactivation days ($M=1.66$, $SD=0.93$). A planned quadratic contrast examining whether the means fit the predicted pattern was also not significant, $F<1$, indicating that this average signal-to-noise measure did not change significantly across the three day inactivation protocol (See Figure 24).

Potential Moderators of Average Signal-to Noise

Muscimol Dose. A 2x2 ANOVA with average signal-to-noise as a within-subjects variable and muscimol dose as a between-subjects variable revealed no significant interaction between inactivation day and dose, $F<1$. Also, there was no significant main effect of dose, $F<1$.

Injection Location. A 2x2 ANOVA with average signal-to-noise as a within-subjects variable and injection location as a between-subjects variable revealed no significant interaction between inactivation day and injection location, $F<1$. Also, there was no significant main effect of injection location, $F<1$.

Direction of change. A 2x2 ANOVA with average signal-to-noise as a within-subjects variable and direction of change in cell activity during inactivation as a between-subjects variable revealed no significant interaction of inactivation day with direction of change , $F<1$. However, there was a significant main effect of direction of change on overall average signal-to-noise ($F(1,19)=7.07$, $p<.05$) such that cells which increased mean firing rate on inactivation days had significantly lower overall average signal-to-noise ($M=1.07$, $SD=0.65$) than did those which decreased activity on inactivation days ($M=1.90$, $SD=0.65$).

Cell Type. A 2x2 ANOVA with average signal-to-noise as a within-subjects variable and cell type as a between-subjects variable revealed no significant interaction of inactivation day and cell type, $F<1$. Also, there was no significant main effect of cell type, $F(4,16) =2.68$, $p>.05$.

Average Target Firing Rate. In order to further investigate the nature of the non-significant changes in average signal-to-noise, which failed to show the same pattern of change during inactivation seen in both peak signal-to-noise measures and correlations among PETH data across the three day inactivation sequence, we assessed the effect of inactivation on target firing rate and background firing rate independently. Although these measures did not vary independently of each other, we measured changes in this way to see if one aspect of the measure was more or less impacted by the effects of thalamic inactivation.

A repeated-measures ANOVA revealed a significant effect of inactivation day on average target firing rate, $F(2,20)=8.01$, $p<.05$. A post-hoc LSD test revealed that target firing rate was significantly higher on pre-inactivation days ($M=14.94$, $SD=10.89$), compared to both inactivation days ($M=6.29$,$SD=5.83$) and post-inactivation days ($M=8.50$,$SD=7.56$), ps $<.05$, which did not differ, $p>.05$. A planned quadratic contrast examining whether the means fit the

predicted pattern was significant, $F(1,20)=7.17$, $p<.05$, the residual contrast was not significant ($F<1$). These data indicate that average target firing rate was lowest on inactivation days compared to pre- and post-inactivation days (See Figure 25).

Average Background Firing Rate. A repeated-measures ANOVA failed to reveal a significant effect of inactivation day on average background firing rate, $F(2,20)=1.06$, $p>.05$, suggesting that background firing rate did not change across the inactivation protocol. However, the means show a trend toward decreasing background firing rate across days, such that background firing rate is highest on pre-inactivation days ($M=9.27$, $SD=7.20$), lower on inactivation days ($M=6.89$, $SD=13.21$), and lowest on post-inactivation days ($M=5.71$, $SD=6.00$), (See Figure 25).

PETH Pattern Correlation. A paired samples t-test revealed that the correlation between event-related pattern of firing was significantly higher on pre-inactivation and post-inactivation days ($M=.66$, $SD=.35$) than between pre-inactivation and inactivation days ($M=.56$, $SD=.33$), $t(20)=2.37$, $p<.05$ (See Figure 26). Thus, event-related pattern of firing was more similar on pre- and post-inactivation days, suggesting the cell was following the same pattern before and after thalamic inactivation, but was shifted significantly during inactivation days.

Potential Moderators of PETH Pattern Correlation

Muscimol Dose. A 2x2 ANOVA with event-related pattern of firing correlation as a within-subjects variable and muscimol dose as a between-subjects variable revealed no significant interaction between the correlation strength and dose, $F(2,18)=2.37$, $p>.05$. Also, there was no significant main effect of dose, $F<1$.

Injection Location. A 2x2 ANOVA with event-related pattern of firing correlation as a within-subjects variable and injection location as a between-subjects variable revealed no significant interaction between the correlation strength and injection location, $F<1$. Also, there was no significant main effect of injection location, $F<1$.

Direction of change. A 2x2 ANOVA with event-related pattern of firing correlation as a within-subjects variable and direction of change in cell activity during inactivation as a between-subjects variable revealed no significant interaction between the correlation strength and the direction of change, $F(1,19)=1.6$, $p>.05$. Also, there was no significant main effect of direction of change, $F<1$.

Cell Type. A 2x2 ANOVA with event-related pattern of firing correlation as a within-subjects variable and cell type as a between-subjects variable revealed no significant interaction between the correlation strength and cell type, $F<1$. Also, there was no significant main effect of cell type, $F(4,16)=1.39$, $p>.05$.

Place Map Pattern Correlation. A paired samples t-test failed to reveal a significant difference in the average correlation between location-specific firing on pre-inactivation and post-inactivation days compared to the correlation between activity on pre-inactivation and inactivation days. , $t(20)=1.09$, $p>.05$, suggesting that the pattern of location-specific firing was not significantly more similar on pre- and post-inactivation days than on pre-inactivation and inactivation days. However, the means trended in the predicted direction, such that average correlation between location-specific firing on pre-inactivation and inactivation days was lower ($M=.66$, $SD=.14$) than the correlation between location-specific firing on pre- and post-inactivation days ($M=.69$, $SD=.16$). (See Figure 27)

Potential Moderators of Place Map Pattern Correlation

Muscimol Dose. A 2x2 ANOVA with location-specific firing correlation as a within-subjects variable and muscimol dose as a between-subjects variable revealed no significant interaction between correlation and dose, $F<1$. Also, there was no significant main effect of dose, $F(2,18)=2.89$, $p>.05$.

Injection Location. A 2x2 ANOVA with location-specific firing correlation as a within-subjects variable and injection location as a between-subjects variable revealed no significant interaction between correlation and injection location, $F<1$. Also, there was no significant main effect of injection location, $F<1$.

Direction of Change. A 2x2 ANOVA with location-specific firing correlation as a within-subjects variable and direction of change in cell activity during inactivation as a between-subjects variable revealed no significant interaction between the correlation strength and direction of change , $F<1$. Also, there was no significant main effect of injection location, $F(1,19)=3.61$, $p>.05$.

Cell Type. A 2x2 ANOVA with location-specific firing correlation as a within-subjects variable and cell type as a between-subjects variable revealed no significant interaction between the correlation strength and cell type , $F<1$. There was, however, a significant main effect of cell type on correlation of location-specific firing, $F(4,16)=5.73$, $p<.05$, such that correlations between location-specific firing for post-reinforcement cells were lower overall ($M=0.43$, $SD=0.09$), compared to all other cell types, including base lever cells ($M=0.74$, $SD=0.09$), movement 1 cells ($M=0.71$, $SD=0.09$), reinforcement excitation cells ($M=0.74$, $SD=0.09$), reinforcement anticipation cells ($M=0.68$, $SD=0.09$).

Location-Specific Place Map Pattern Correlation. When only those cells which exhibited location-specific activity (n=7; See Figure 28 for example) were included in analyses, a paired samples t-test revealed only a marginally significant difference in the average correlation between location-specific firing on pre-inactivation and post-inactivation days compared to the correlation between activity on pre-inactivation and inactivation days , $t(6)=2.25$, $p=.07$, suggesting that the pattern of location-specific firing was marginally more similar on pre- and post-inactivation days than on pre-inactivation and inactivation days. However, the means trended in the predicted direction, such that average correlation between location-specific firing on pre-inactivation and inactivation days was lower ($M=.66$, $SD=.17$) than the correlation between location-specific firing on pre- and post-inactivation days ($M=.77$, $SD=.11$).

Similarly, a paired samples t-test revealed a marginally significant difference in the average correlation between location-specific firing on pre- and post-inactivation days compared to the correlation between activity on inactivation and post-inactivation days, $t(6)=2.15$, $p=.08$. The means again trended in the predicted direction, such that average correlation between location-specific firing on inactivation and post-inactivation days was lower ($M=.70$, $SD=.10$) than the correlation between location-specific firing on pre- and post-inactivation days.

A planned quadratic contrast revealed that the pattern of mean correlations fit the predicted pattern, such that the average correlation between location-specific firing on pre- and post-inactivation days was significantly higher than the average correlation between location-specific firing on pre-inactivation and inactivation days, as well as on inactivation and post-inactivation days, $F(1,6)=10.70$, $p<.05$, the residual contrast was not significant ($F<1$) (See Figure 29). These data suggest the pattern of location-specific firing was more similar on days before and after inactivations than on days with inactivations.

DISCUSSION

The type of general disruption of prefrontal cortical firing patterns observed during thalamic inactivation sessions is consistent with the hypothesis that central thalamic nuclei are indeed critical in modulating and tuning the activity of corticocortical circuits.

The main findings of this research were that the signal-to-noise properties of prefrontal cells were significantly degraded when thalamic connections were temporarily disrupted my muscimol inactivation. This was evident in the significant decrease in peak Z-scores representing maximal event-related firing surrounding critical behavioral events in the DNMTP task, as well as the significantly stronger correlation between the shape of PETH activity on pre- and post-inactivation days as compared to pre-inactivation and inactivation days. Even those measures of event-specific firing which did not reach significance trended in the predicted direction, suggesting that even those effects which were small or affected by wide variability were all following the same general pattern.

Taken together, these findings suggest that the ability of cortical cells to accurately represent the key elements of the behavioral task, as assessed by two distinct measures, is dependent on intact thalamocortical communication.

Continuing to assess the nature of prefrontal coding of behavior, memory and motivation during the dynamic DNMTP task, we have built on previous work in our lab in which consistent cell types were identified by their signature changes in firing activity surrounding discrete events in the task (Mair et al., 2015; Onos et al., manuscript in preparation). Here we identified several of the unique response types initially laid out in previous recording studies, illustrating a high

degree of consistency across subjects in the patterns of activity which prefrontal cortical cells exhibit in relation to the same behavioral task. Having characterized the cell responses in the same way, and identified their critical periods of activity based on these same earlier studies, we have gone on to demonstrate a clear pattern in which these same response properties begin to lose their behavioral specificity when central thalamus is temporarily inactivated. These results suggest not only that we have accurately described the way prefrontal cells respond to the task under normal conditions, but also the way in which these same cells are impaired in this function when thalamocortical communication is disrupted.

These findings are consistent with the literature suggesting thalamic nuclei may serve a gating function, modulating the action of prefrontal cortical neurons by regulating corticothalamocortical circuits (León-Domínguez, Vela-Bueno, Froufé-Torrex, & León-Carrión, 2013; Saalmann, 2014; Schiff, 2008; Schiff et al., 2013). If central thalamus is in fact modulating the firing properties of cortical neurons, we would expect to see exactly the type of disruption observed here when thalamic input is temporarily cut off. The fact that cortical neurons are involved in multiple networks, and communicating with numerous other cortical regions, with and without the intervention of thalamic nuclei (Sherman & Guillery, 2011), explains why we failed to observe a total lack of event-related response, but rather saw similar response patterns persist, but with significantly degraded signal-to-noise properties.

The significant disruption of measures signal-to-noise at maximal firing rate surrounding key events (peak signal-to-noise), as well as the significant deviation in the moment-to-moment pattern of firing across the 10s windows containing the critical events (PETH pattern correlation) were consistent across drug doses, injection sites, cell types, and cells which increased or decreased activity on inactivation days. The lack of any significant interaction effects indicates a

strong and consistent effect of thalamic inactivation, whereby the specificity of cell activity to critical task events is disrupted irrespective of all other potential moderating variables measured. That effects are maintained in both cells which increase activity during inactivation and those which decrease activity suggests that the influence of thalamus on cortical firing properties is not driven merely by excitatory or inhibitory mechanisms, but by a complex interplay of both types of synaptic control.

This finding is consistent with recent findings using optogenetic methods to assess the types of synaptic activity involved in thalamocortical circuits (Cruikshank, Urabe, Nurmikko, & Connors, 2009; Cruikshank et al., 2012; Crandall, Cruikshank, & Connors, 2015), which indicate excitability in cortical neurons being altered both by direct excitatory synapses as well as indirect inhibitory synapses, both types being driven by stimulation of central thalamus. If the modulation of these circuits does in fact rely on excitatory output from thalamus driving both inhibitory and excitatory connections within corticocortical networks, one would expect that temporarily removing the initial excitatory input from thalamus would lead to decreased excitability in certain cells whose direct input had been cut off, but increased excitability in those cortical neurons which were typically inhibited as a result of feed-forward connections involving inhibitory interneurons being driven by thalamic synapses. That we observed both types of changes in excitation of prefrontal neurons is consistent with these networks as they have been described, as it is quite possible we were simultaneously recording from both excitatory and inhibitory interneurons being affected in opposite directions by the inactivation of central thalamus, with the one common effect being that signal-to-noise characteristics were significantly reduced in both types of neuron.

Place Map Correlation and Spatial Coding Properties

The effects of thalamic inactivation on spatial coding properties were somewhat less clear, but the data indicate that, at least in those cells which do appear to respond to spatial context as well as events in the task, the same degradation in signal-to-noise properties seen in peak-to-background firing rates and the correlations of PETH data seem to carry over to the cells' place coding characteristics as well. These analyses were limited by the small number of cells which were accurately tracked across all 3 days and also showed place coding properties, but the significant contrast among correlation coefficients does fit the predicted pattern, with the relationship between pre-inactivation and post-inactivation spatial heat maps being the strongest. This indicates that the pattern of activity as it related to spatial location was significantly more related before and after the inactivation, and significantly less consistent when thalamic input was temporarily disrupted. This supports the evidence seen in PETH correlations indicating particular pattern of activity which falls apart when thalamus is inactivated and returns on the following day.

Signal-to-Noise Measures and PETH Pattern Correlation

The major significant results pertaining to neurons' signal-to-noise properties discussed above relate to two of the three ways in which the degree to which a cell's activity reflected critical task events was affected by thalamic inactivation. Peak Z-scores, as a measure of the relationship between maximal activity during these events compared to the average activity immediately preceding and following said events, provides an estimate of signal-to-noise characteristics in the cell's pattern of activity. However, these peak scores only consider the absolute highest rate of firing, and exclude the rise and fall of activity around the peak bin.

Furthermore, though cells are initially typed by the timing of their activity, and peak Z-scores are taken from the single events which best characterize that critical increase in activity, it is possible for maximal firing to occur near the target window identified in previous research (Onos et al., manuscript in preparation), but not necessarily within it. The strength of the automated approach is that the peak firing is totally objective, and immune to any type of bias or human error. However, in using such a standardized analysis, it is possible to miss some of the properties of the cell response which define its type, and which potentially more completely describe the way in which it changes when thalamic input is cut off.

In order to complement the automated measure of maximal firing, we also calculated the more comprehensive average signal-to-noise metric. This had the advantage of including the entirety of a cell's activity over the session, and breaking it into two distinct categories: firing which occurred within the predetermined time window relevant to that response type, and firing which occurred without. In this way no data was excluded, and all of the activity which should (based on a priori timing categories established in previous research) correspond to the event was compared to all of the rest of the cell's activity.

Despite these advantages, the lack of significant effects suggests that either there was no effect of inactivation on signal-to-noise properties of prefrontal cells or this metric was somehow missing it. Given the strong effects seen when measuring changes in peak Z-scores as well as comparing correlation strengths between pairs of inactivation days, it seems unlikely that there was actually no effect of the manipulation whatsoever. Rather, it is possible that by expanding the target and background window so far beyond peak measures, we simply made too much room for variability in the vast amount of data analyzed.

In order to further elucidate this issue, we considered background mean firing rate and target mean firing rate as separate variables (though they cannot truly vary independently). Here we see that the changes in average target firing (our measure of event-specific signal) are in fact altered significantly by the inactivation of thalamus, while the average background firing simply continues to decline across all three days of the protocol. As overall firing goes down, it necessarily limits the possible amount of target firing rate. That target firing rate still recovers significantly on post-inactivation days, even given the overall decline in cell activity, suggests this measure on its own may be more accurately representing the pattern of change in signal-to-noise across the inactivation protocol. While the average signal-to-noise measure failed to demonstrate significant inactivation effects on its own, the change observed in target firing rate, as well as the effects seen in the other measures of event-specific activity, all support the same pattern of change during thalamic inactivation.

Having measured effects on target-to-background ratios which estimate signal-to-noise, we further investigated the shape, or pattern, of event-related activity by addressing the entire period surrounding each critical event with a moment-to-moment comparison of each 200ms bin on either side of the labeled task event. This was accomplished by correlating the key PETH windows with one another, such that each bin in the pre-inactivation PETH was compared against its counterpart in the inactivation and post-inactivation PETHs. By correlating the entire window with its corresponding window during and after inactivation we were able to address the entire pattern of change across days. We hypothesized that pre-inactivation PETH values should be strong predictors of post-inactivation PETH values because they were hypothetically measuring the same cell during the same task, in the absence of outside manipulation. This was indeed supported by strong correlations between pre- and post-inactivation activity across the

PETH windows, which were, as predicted, significantly stronger than those between pre-inactivation and inactivation days. This finding demonstrates that, as signal-to-noise properties defined by maximal firing degrade, so too does the entire shape of the cell's firing over time. The pattern of the cell's firing response around critical task events falls apart when thalamus is inactivated, only weakly resembling the distribution of activity before and after the manipulation.

This correlation data, alongside significant changes in peak signal-to-noise as well as average target firing rates, all support the existing literature pointing to central thalamus as a mechanism for modulating the firing of prefrontal cells to shape their activity as it relates to key elements in the animal's planning and goal-directed action. When thalamus's contribution to the corticothalamocortical circuits required for this type of behavior is removed, the ability of cortical neurons to represent learned rules and perceived rewards is clearly disrupted.

Performance Accuracy

The lack of significant inactivation effects on proportion of correct responses within the targeted data indicates the unilateral manipulation was not associated with behavioral impairments which would suggest a spread of the drug to the opposite hemisphere or other collateral damage. This suggests the cortical activity recorded before and after inactivation days was indicative of the functions in the opposite, spared hemisphere. This provides us with a measure of how cortical neurons with intact, healthy thalamic communication code for the events within the DNMTP task, and suggests that any changes observed in the way these cells change their activity around the events in the task are a result of the temporary severing of communications with central thalamus.

These results suggest that the effects observed in the hemisphere ipsilateral to the inactivation site are similar to those which contributed to impairment on related tasks in previous research when performed bilaterally (Mair et al., 1998; Mair, Onos, & Hembrook, 2011). Bilateral inactivation of thalamus caused significant impairment on a number of tasks dependent on spatial working memory and basic decision making which relied on intact spatial memory.

Here, by dissociating the behavioral impairment from changes in neural activity by using a unilateral manipulation, we provide evidence for the processes which were likely disrupted in both hemispheres in previous experiments, leading to significant task impairment. That performance was not significantly altered by unilateral inactivation indicates the intact hemisphere allowed the animal to complete the task based on previous training, while observations in the manipulated hemisphere provided a glimpse of the exact type of disruption in coding properties which could produce just the type of deficits observed in the previous bilateral studies.

The initial analyses of our data did reveal a significant impairment of performance accuracy when all inactivations were included (See Appendix D). However, this finding, along with evidence of considerable damage to the tissue in the subject receiving the most injections (See Figure 19), lead to concern that these effects were a result not of the temporary inactivation itself, but rather of long term changes in the function of targeted regions being caused by the effects of chronic intracerebral injections. These could have resulted from chronic exposure to the muscimol itself as demonstrated in certain cases (Honegger, Pardo & Monnet-Tschudi, 1998; Lomber, 1999; Malpeli, 1999; Xu et al., 2000), or conceivably from additive effects of repeated exposure to the injection procedure itself, with repeated penetrations of the internal injection cannula and forced infusion of saline vehicle, regardless of drug effects.

The presence of significant performance impairment, along with evidence of collateral damage which, should similar effects extend across the midline (which was not clearly in evidence in the histology, but could well have happened given the extent of unintended damage seen only in the case of the largest number of injections) could produce this type of behavioral impairment, raised enough questions about the nature of the data collected form later procedures that we decided to exclude them. In the absence of a clear cut-off point, or indisputable evidence of when exactly damage began to accumulate in the chronically injected subjects, we made the decision to use the median number of injections given to all subjects as the number of protocols from which data would be analyzed. In this way all subjects could be evaluated on more equal footing, and we could be more certain that the effects observed in one animal were comparable to those seen in another, without the threat of contamination caused by multiple intervening injections in certain cases.

The findings discussed here support the proposed role of central thalamus, and MD in particular, as a higher order modulator of cortical activity (Sherman & Guillery, 2011; Parnadeau et al., 2013) serving to tune the firing of mPFC neurons in order to code contextual stimuli and behavioral events in a way which could potentially improve the accuracy with which the animal represents and responds to its environment. The significant reduction in signal-to-noise properties of behaviorally correlated cell firing, in the absence of parallel decreases in correct responding or mean firing rate, indicates a specific effect of thalamic inputs to mPFC beyond merely exciting or inhibiting cortical firing. These data suggest that the excitatory glutamatergic projections from central thalamic nuclei including MD, likely through their action on both inhibitory and excitatory interneurons (As in Cruikshank et al., 2009; Cruikshank et al., 2012),

are affecting the relationship of neuron firing rates to the actions and outcomes which are most relevant to the animal during performance of the DNMTP task.

The elevated clarity of neural signal tied to specific events when thalamic input is intact, and the relative increase of background firing when it is inactivated, could indicate that thalamic modulation helps these cortical cells more accurately represent both key features in the environment as they occur (as seen in cells which appear to encode the delivery of water reinforcement after the completion of a rewarded action) as well as accurately change their pattern of activity to signal coming changes in the task, presumably based on past experience (as seen in cells which increase firing rate in anticipation of reinforcement delivery).

The absence of any significant interactions supports a general effect on all identified cell types, indicating that, to some degree, all of the coding properties of the medial prefrontal neurons recorded rely on intact thalamocortical circuitry to retain their ability to represent specific information by significantly altering their rate of activity compared to background levels. These data cannot determine for certain how exactly the function of these neurons encodes information about the task and environment, but they are certainly consistent with the hypothesis that the cells maintain a steady rate of firing at all times, only producing significant, targeted increases or potentially decreases, although this type of response was not recorded here, such cells are present in other prefrontal recording experiments, (see Onos et al., manuscript in preparation).

Limitations and Future Directions

While the findings of this experiment are consistent with the hypothesis that central thalamus plays a critical role in shaping and sharpening the peak signal-to-noise of mPFC

neurons, further research is necessary to determine the exact routes and mechanisms involved in this modulation.

It is possible that discrete classes of neurons could be identified by properties in their waveforms and timing in order to separate putative inhibitory interneurons from pyramidal cells (As in Cruikshank et al., 2009; Cruiskshank et al., 2012). While our methods involved driving across multiple layers of cortex and presumably through many types of cells, our recordings lacked the resolution to parse these differences. Preliminary findings suggest no clear relationship between the waveforms widths and firing rates of the cells recorded and their behavioral specificity or topographical location, but further experiments using smaller and more carefully guided tetrode arrays, and refined data filtering and processing which could better identify small differences in waveform shape and timing, could shed more light on this question.

In order to more fully understand exactly how thalamus is influencing mPFC, it would also be of interest to experiment with low level excitatory stimulation of thalamic nuclei in addition to temporary inactivation. Previous findings indicate high levels of stimulation can disrupt thalamic-dependent tasks and functions, but that very minimal stimulation can actually improve performance in these areas (Duan et al., 2015; Mair & Hembrook, 2008; Mair, Onos, & Hembrook, 2011). It would be possible to conduct both types of manipulation within single subjects using optogenetic techniques (As in Cruikshank et al., 2009; Cruikshank et al., 2012) to alternate between inhibition and stimulation of the critical regions in thalamus while recording the impact of these manipulations on cortical firing properties. This two-pronged approach could likely produce a fuller understanding of exactly what function central thalamus plays in the corticothalamocortical circuitry critical to working memory and goal-directed action for the DNMTP task. This would also likely allow us to target more discrete regions with more

accuracy and reliability, as the diffusion of muscimol is not entirely predictable in its time course or spread of inactivation (Arikan et al., 2002; Edeline, Hars, Hennevin, & Cotillon, 2002). More focused and versatile inactivation methods, including optogenetic techniques, would likely improve the regional specificity of our effects, further elucidating the role of more discrete nuclei in thalamus in modulating cortical coding properties.

Another area in which to expand upon the current work involves the time course of manipulations and recording. That mean firing rate and background firing rate were seen to decline across all three days in many cases raises questions about what mechanisms are causing this steady loss of activity. It is possible that our ability to record all of the activity from a single cell was interfered with the longer the tetrode array remained in one area, potentially obstructed by early gliosis or other organic accumulation on the recording surface. It is also impossible to rule out the possibility of the tetrode shifting enough over time to move further from the source cells, or simply that the cell itself is becoming less active or even dying off due to the mechanical trauma of the nearby implant being driven through the tissue around it.

It is also possible, however, that the muscimol injected, having a high affinity for $GABA_A$ receptors, has simply failed to completely leave the infusion site. While current literature suggests the drug should cease being active well before the 24 hour mark (Edeline et al., 2002), it is difficult to categorically rule out this possibility without further investigation, especially given that previous work with this type of inactivation has allowed considerably more time between injections than was sometimes allowed in our subjects, raising questions about additive effects of chronic infusions (Mair & Hembrook, 2011).

In order to more thoroughly address these concerns, it would be beneficial to allow more time between injections for each subjects record cells for an additional day following inactivation in order to observe changes, if any, on the fourth day which could indicate the initial post-inactivation signal was lowered by lingering effects of the drug or by some less controllable aspect of the procedure. This was attempted in the present study, but we were unable to track a single cell into the fourth day, and thus could not assess these differences. While this may indicate that four days is simply too long to accurately record from one tetrode, or that it is long enough for cells to begin dying off, we cannot be certain without further investigation into this area.

Further research specifically on those cells which show clear location-specific firing properties also stands to expand our understanding of how this aspect of prefrontal coding is altered when thalamus is removed from the circuit. In the current study, cells were identified based on waveform and cluster properties, as well as their degree of behavioral specificity as measured by PETH data around key task events. Those cells which showed the strongest and most readily identifiable responses along these specific metrics were the ones tracked across the three day protocol and observed for effects of thalamic inactivation. If, instead, cells which showed clear location-specific firing were identified and targeted for the inactivation protocol, we would be able to assemble a more complete body of data regarding how this unique type of prefrontal neuron responds to the temporary disruption of thalamocortical circuits. The data already analyzed in the current research suggest further experiments would yield similar results, with place coding properties falling apart during thalamic inactivation and returning to their original pattern in the days following injection, in the same way behavioral measures of signal-to-noise properties were seen to change here.

Implications

Central thalamus has long been a focus of research on the nature of memory and its associated disorders. Effects of thalamic damage are wide-ranging and often severe, they can be seen both in human pathology (McEntee, Biber, Perl, & Benson, 1976; Squire, Amaral, Zola-Morgan, Kritchevsky, & Press, 1989; van der Werf et al., 2003) and in experimental lesions in non-human animals (Aggleton & Mishkin, 1983; Mair & Hembrook, 2008). The global amnesia seen in humans with damage to thalamus can extend to multiple modalities and categories of memory, and the effects produced by even relatively small, focal lesions in this region are capable of disrupting memory and behavior well beyond the effects seen in comparable lesions to prefrontal cortex (Harrison & Mair, 1996). The observation that even minimal damage to central thalamus can produce such drastic alterations in memory function and the type of response planning and goal-directed action which rely on working memory but have long been associated with prefrontal executive function points to this region as critical for far more complex functions than the early textbook description as a sensory relay (Starzl & Magoun, 1951) would suggest.

Furthermore, central thalamus, and its communication with prefrontal regions, is implicated in pervasive disorders not only of memory, but of thought (León-Domínguez, Vela-Bueno, Froufé-Torrex, & León-Carrión, 2013; Saalmann, 2014; Schiff, 2008; Schiff et al., 2013), with dysfunction or damage in the region being tied to schizophrenia, and incoherence in thalamocortical networks associated with a number of cognitive disruptions.

The research discussed here presents a new and powerful element in the ongoing understanding of central thalamus's role less as a single critical component which, when absent,

causes the loss of thalamus-specific abilities, and more as a critical link in a broad network of corticothalamocortical circuits involved in everything from sensory processing to memory-dependent planning and adaptive action. This is a small subcortical structure which, by virtue of being densely interconnected with regions like medial prefrontal cortex and hippocampal formation (Viana, DiPrisco & Vertes, 2006, Vertes et al. 2007), has the potential to modulate the activity of neurons at any stage of communication among these areas, and thus affect the processing of information related to memory, navigation, rule learning, reward salience, and goal-directed action. In this way, central thalamus can be at least partially responsible for a huge number of the unique elements of sensation, perception, memory and behavior which are so often ascribed to other brain regions more directly linked to the corresponding output.

Human data suggest this same type of function may be involved in regulating thalamocortical coherence in functions involved in consciousness and cognition as well as memory, pointing to this tiny subcortical structure as a critical component of systems which span the nervous system and process vast amounts of information in order to generate the most adaptive response available. The findings presented here have characterized important aspects of the nature of thalamocortical projections as they relate to adaptive behavior including rule learning, response-planning, and working memory. However, this is only scratching the surface of the dense, complex interconnections among these regions, and further investigation along the lines described here could create a much more detailed picture of how these systems contribute to higher order cognitive function, paving the way for new and more effective treatments when these functions are compromised.

Beyond the potential for diagnostic and therapeutic purposes, the effects measured on the signal-to-noise properties of prefrontal cortical neurons support one key piece of evidence for an

expanded role of central thalamus, suggesting that functions once thought to depend on prefrontal cortex are meaningfully impacted by thalamic communication. This supports the conception of thalamus as serving a gating or modulating function (Cruikshank et al., 2009; Sherman & Guillery, 2011; Parnadeau et al., 2013) whereby it can shape the pattern of activity in the cortical circuits in which it acts as a relay, tuning their function in a way which most accurately reflects the most relevant aspects of an organism's environment and history.

By tuning the response properties of cortical neurons in relation to events defined by timing, reward, and spatial memory traces, this region can incorporate critical information from diverse brain regions and thus maximize the degree to which cortex accurately prepares the organism to produce the most adaptive response in any given situation. By modulating the activity of cortex, and theoretically any other systems which has reciprocal connections with it, central thalamus is uniquely positioned at the center of a number of vitally important adaptive functions, and these data only represent one key step in the very beginning of a systems-level understanding of how the brain makes sense of all of the information around us to generate the most effective action for any given circumstance.

REFERENCES

Aggleton, J. P., Hunt, P. R., Nagle, S., & Neave, N. (1996). The effects of selective lesions within the anterior thalamic nuclei on spatial memory in the rat. *Behavioural brain research*, *81*(1), 189-198.

Aggleton, J. P., & Mishkin, M. (1983). Memory impairments following restricted medial thalamic lesions in monkeys. *Experimental Brain Research*, *52*(2), 199-209.

Amat, J., Baratta, M. V., Paul, E., Bland, S. T., Watkins, L. R., & Maier, S. F. (2005). Medial prefrontal cortex determines how stressor controllability affects behavior and dorsal raphe nucleus. *Nature neuroscience*, *8*(3), 365-371.

Arikan, R., Blake, N. M., Erinjeri, J. P., Woolsey, T. A., Giraud, L., & Highstein, S. M. (2002). A method to measure the effective spread of focally injected muscimol into the central nervous system with electrophysiology and light microscopy. *Journal of neuroscience methods*, *118*(1), 51-57.

Bailey, K.R., & Mair, R.G. (2005) Lesions of specific and nonspecific thalamic nuclei affect prefrontal cortex-dependent aspects of spatial working memory. *Behavioral Neuroscience*, *119*(2), 410-419.

Braak H. & Braak E.(1998). Evolution of neuronal changes in the course of Alzheimer's disease. *J. Neural. Transm.*, *53*, 127–40.

Burk, J.A., & Mair, R.G. (1998). Thalamic amnesia reconsidered: Excitotoxic lesions of the intralaminar nuclei, but not the mediodorsal nucleus, disrupt place delayed matching-to-sample performance in rats (*Rattus norvegicus*).*Behavioral Neuroscience*, *112*(1), 54-67.

Bussey, T. J., Muir, J. L., Everitt, B. J., & Robbins, T. W. (1997). Triple dissociation of anterior cingulate, posterior cingulate, and medial frontal cortices on visual discrimination tasks using a touch screen testing procedure for the rat. *Behavioral Neuroscience*, *111*, 920-936.

Cardinal, R. N., Parkinson, J. A., Hall, J., & Everitt, B. J. (2002). Emotion and motivation: the role of the amygdala, ventral striatum, and prefrontal cortex. *Neuroscience & Biobehavioral Reviews*, *26*(3), 321-352.

Chen, Q., Olney, J. W., Lukasiewicz, P. D., Almli, T., & Romano, C. (1998). Ca2+-independent excitotoxic neurodegeneration in isolated retina, an intact neural net: a role for Cl− and inhibitory transmitters. *Molecular pharmacology*,*53*(3), 564-572.

Chudasama Y. & Robbins T.W. (2003). Dissociable contributions of the orbitofrontal and infralimbic cortex to pavlovian autoshaping and discrimination reversal learning: further evidence for the functional heterogeneity of the rodent frontal cortex. *J. Neurosci., 23*, 8771–80.

Crandall, S. R., Cruikshank, S. J., & Connors, B. W. (2015). A Corticothalamic switch: Controlling the thalamus with dynamic synapses. *Neuron*, *86*(3), 768-782.

Cruikshank, S. J., Ahmed, O. J., Stevens, T. R., Patrick, S. L., Gonzalez, A. N., Elmaleh, M., & Connors, B. W. (2012). Thalamic control of layer 1 circuits in prefrontal cortex. *The Journal of Neuroscience*, *32*(49), 17813-17823.

Cruikshank, S. J., Urabe, H., Nurmikko, A. V., & Connors, B. W. (2010). Pathway-specific feedforward circuits between thalamus and neocortex revealed by selective optical stimulation of axons. *Neuron*, *65*(2), 230-245.

Dempsey E.W. & Morison R.S. (1942). The production of rhythmically recurrent cortical potentials after localized thalamic stimulation. *Am. J. Physiol., 135*, 293– 300.

Devinsky, O., Morrell, M. J., & Vogt, B. A. (1995). Contributions of anterior cingulate cortex to behaviour. *Brain*, *118*(1), 279-306.

Dias, R., & Aggleton, J. P. (2000). Effects of selective excitotoxic prefrontal lesions on acquisition of nonmatching-and matching-to-place in the T-maze in the rat: Differential involvement of the prelimbic–infralimbic and anterior cingulate cortices in providing behavioural flexibility. *European Journal of Neuroscience*, *12*(12), 4457-4466.

Dolleman-van der Weel, M.J., Lopes da Silva, F.H. & Witter, M.P, (1997). Nucleus reuniens modulates activity in hippocampal field CA1 through excitatory and inhibitory mechanisms, *J. Neurosci., 17*, 5640-5650.

Dolleman-van der Weel, M.J., Morris, R.G. & Witter, M.P. (2009). Neurotoxic lesions of thalamic reuniens or mediodorsal nucleus in rats affect nonmnemonic aspects of water maze learning. *Brain Structure Function, 213*, 329-42.

Duan, A. R., Varela, C., Zhang, Y., Shen, Y., Xiong, L., Wilson, M. A., & Lisman, J. (2015). Delta Frequency Optogenetic Stimulation of the Thalamic Nucleus Reuniens Is Sufficient to Produce Working Memory Deficits: Relevance to Schizophrenia. *Biological psychiatry*.

Edeline, J. M., Hars, B., Hennevin, E., & Cotillon, N. (2002). Muscimol diffusion after intracerebral microinjections: a reevaluation based on electrophysiological and autoradiographic quantifications. *Neurobiology of learning and memory*, *78*(1), 100-124.

Eichenbaum, H., Clegg, R. A., & Feeley, A. (1983). Reexamination of functional subdivisions of the rodent prefrontal cortex. *Experimental neurology*, *79*(2), 434-451.

Funahashi, S., Bruce, C. J., & Goldman-Rakic, P. S. (1989). Mnemonic coding of visual space in the monkey's dorsolateral prefrontal cortex. *Journal of neurophysiology*, *61*(2), 331-349.

Fuster, J. M., & Alexander, G. E. (1971). Neuron activity related to short-term memory. *Science*, *173*(997), 652-654.

Goel, V. (2007). Anatomy of deductive reasoning. *Trends in cognitive sciences*, *11*(10), 435-441.

Gold, J.J. & Squire, L.R. (2005). Quantifying medial temporal lobe damage in memory-impaired patients. *Hippocampus*, *15*, 79–85.

Goldman-Rakic, P. S. (1987). Circuitry of primate prefrontal cortex and regulation of behavior by representational memory. *Comprehensive Physiology*.

Groenewegen, H.J. & Berendse, H.W. (1994). The specificity of the "nonspecific" midline and intralaminar thalamic nuclei. *Trends Neurosci.*, *17*, 52–57.

Harrison, L. M., & Mair, R. G. (1996). A comparison of the effects of frontal cortical and thalamic lesions on measures of spatial learning and memory in the rat. *Behavioural brain research*, *75*(1), 195-206.

Hembrook J.R. & Mair R.G. (2010). Lesions of reuniens and rhomboid thalamic nuclei impair radial maze win-shift performance. *Hippocampus*, *21*(8), 815-826.

Honegger, P., Pardo, B., & Monnet-Tschudi, F. (1998). Muscimol-induced death of GABAergic neurons in rat brain aggregating cell cultures.*Developmental brain research*, *105*(2), 219 225.

Hoover, W.B. & Vertes, R.P. (2007). Anatomical analysis of afferent projections to the medial prefrontal cortex in the rat, *Brain Struct. Funct.*, *212*, 149–179.

Iancu, T. C. (1992). Ferritin and hemosiderin in pathological tissues. *Electron microscopy reviews*, *5*(2), 209-229.

Isseroff, A., Rosvold, H. E., Galkin, T. W., & Goldman-Rakic, P. S. (1982). Spatial memory impairments following damage to the mediodorsal nucleus of the thalamus in rhesus monkeys. *Brain Research*, *232*(1), 97-113.

Jasper, H.H. (1960). Sensory information and conscious experience, in: Jasper, H.H., Descarries, L., Castellucci, V.F. & Rossignol, S. (Eds.) Consciousness: At the frontiers of neuroscience, Advances in Neurology, Vol. 77, Lippincott-Raven, Philadelphia, PA (1998), 33-48.

Jones E.G. (1985). The thalamus. New York: Plenum.

Jones E.G. & Leavitt R.Y. (1974). Retrograde axonal transport and the demonstration of non specific projections to the cerebral cortex and striatum from thalamic intralaminar nuclei in the rat, cat and monkey. *J. Comp. Neurol.*, *154*, 349–377.

Kesner, R. P., Hunt, M. E., Williams, J. M., & Long, J. M. (1996). Prefrontal cortex and working memory for spatial response, spatial location, and visual object information in the rat. *Cerebral Cortex*, *6*(2), 311-318.

León-Domínguez, U, Vela-Bueno, A., Froufé-Torrex, M., León-Carrión, J., 2013. A chronometric functional sub-network in the thalamo-cortical system regulates the flow of neural information necessary for conscious cognitive processes. Neuropsychologia 51, 1336-1349.

Llinás, R. R., Ribary, U., Jeanmonod, D., Kronberg, E., & Mitra, P. P. (1999). Thalamocortical dysrhythmia: a neurological and neuropsychiatric syndrome characterized by magnetoencephalography. *Proceedings of the National Academy of Sciences*, *96*(26), 15222-15227.

Lomber, S. G. (1999). The advantages and limitations of permanent or reversible deactivation techniques in the assessment of neural function.*Journal of neuroscience methods*, *86*(2), 109-117.

Mair, R.G., Burk, J.A. & Porter, M.C. (1998). Lesions of the frontal cortex, hippocampus, and intralaminar nuclei have distinct effects on remembering in rats. *Behavioral Neuroscience*, *112*, 772-792.

Mair, R.G., & Hembrook, J.R., (2008). Memory enhancement with event-related stimulation of the rostral intralaminar thalamic nuclei. *J. Neurosci.*, *28*, 14293-14300.

Mair, R. G., Koch, J. K., Newman, J. B., Howard, J. R., & Burk, J. A. (2002). A double dissociation within striatum between serial reaction time and radial maze delayed nonmatching performance in rats. *J Neuroscience*, *22*, 6756–6765.

Mair, R. G., Miller, R. L., Wormwood, B. A., Francoeur, M. J., Onos, K. D., & Gibson, B. M. (2015). The neurobiology of thalamic amnesia: contributions of medial thalamus and prefrontal cortex to delayed conditional discrimination.*Neuroscience & Biobehavioral Reviews*, *54*, 161-174.

Mair, R.G., Onos, K.D., & Hembrook, J.R. (2011). Cognitive activation by central thalamic stimulation: The Yerkes-Dodson law revisited. *Dose-Response*, *9*(3), 313-331.

Malpeli, J. G. (1999). Reversible inactivation of subcortical sites by drug injection. *Journal of neuroscience methods*, *86*(2), 119-128.

McEntee, W. J., Biber, M. P., Perl, D. P., & Benson, D. F. (1976). Diencephalic amnesia: a reappraisal. *Journal of Neurology, Neurosurgery & Psychiatry*, *39*(5), 436-441.

Miller, E. K., Freedman, D. J., & Wallis, J. D. (2002). The prefrontal cortex: categories, concepts and cognition. *Philosophical Transactions of the Royal Society B: Biological Sciences*, *357*(1424), 1123-1136.

Miller, R.L.A., Onos, K.D., Francoeur, M.J., Wormwood, B.A., Smedley, E.B., Theriault, C.J., Ryder, E.E., Gibson, B.M., & Mair, R.G. (2014, November). *Encoding of information about action and context by medial thalamus in the rat: Comparisons to prefrontal cortex.* Poster presented at the annual Society for Neuroscience Conference, Washington, D.C.

Morgane, P. J., Galler, J. R., & Mokler, D. J. (2005). A review of systems and networks of the limbic forebrain/limbic midbrain. *Progress in neurobiology*, *75*(2), 143-160.

Moruzzi, G. & Magoun, H.W. (1949). Brain stem reticular formation and activation of the EEG. *Electroencephalography and Clinical Neurophysiology*, *1*, 455-473.

Nyberg, L., Marklund, P., Persson, J., Cabeza, R., Forkstam, C., Petersson, K. M., & Ingvar, M. (2003). Common prefrontal activations during working memory, episodic memory, and semantic memory. *Neuropsychologia*, *41*(3), 371-377.

Onos, K.D., Francoeur, M.J., Wormwood, B.A., Miller, R.L.A., Gibson, B.M., & Mair, R.G.(2014).Medial prefrontal neurons encode a common core of information required for flexible goal-directed behavior. Manuscript in preparation.

Parnaudeau, S., O'Neill, P.K., Bolkan, S.S., Ward, R.D., Abbas, A.I., Roth, B.L., Balsam, P.D., Gordon, J.A., & Kellendonk, C. (2013). Inhibition of mediodorsal thalamus disrupts thalamofrontal connectivity and cognition. *Neuron 77,* 1151-1162.

Porter, M.C., Koch, J., & Mair, R.G. (2001) Effects of reversible inactivation of thalamo-striatal circuitry on delayed matching trained with retractable levers. *Behavioural Brain Research*, *119*(1), 61-69.

Poulet, J. F., Fernandez, L. M., Crochet, S., & Petersen, C. C. (2012). Thalamic control of cortical states. *Nature neuroscience*, *15*(3), 370-372.

Rafal, R. D., & Posner, M. I. (1987). Deficits in human visual spatial attention following thalamic lesions. *Proceedings of the National Academy of Sciences*, *84*(20), 7349-7353.

Ragozzino, M. E., Adams, S., & Kesner, R. P. (1998). Differential involvement of the dorsal anterior cingulate and prelimbic–infralimbic areas of the rodent prefrontal cortex in spatial working memory. *Behavioral neuroscience*, *112*(2), 293.

Rowland, D. C., Yanovich, Y., & Kentros, C. G. (2011). A stable hippocampal representation of a space requires its direct experience. *Proceedings of the National Academy of Sciences*, *108*(35), 14654-14658.

Saalmann, Y.B., 2014. Intralaminar and medial thalamic influence on cortical synchrony, information transmission and cognition. Front. Syst. Neurosci. 8:83.

Sarnthein, J., Morel, A., Von Stein, A., & Jeanmonod, D. (2005). Thalamocortical theta coherence in neurological patients at rest and during a working memory task. *International journal of psychophysiology*, *57*(2), 87-96.

Schiff, N.D. (2008). Central thalamic contributions to arousal regulation and neurological disorders of consciousness. *Ann. N.Y. Acad. Sci*., *1129*, 105– 118.

Schiff, N.D., Shah, S.A., Hudson, A.E., Nauvel, T., Kalik, S.F., Purpura, K.P.,2013. Gating of attentional effort through the central thalamus. J. Neurophysiol. 109, 1152-1163.

Shallice T. (1982) Specific impairments of planning. *Philos. Trans. R. Soc. Lond. B. Biol. Sci.*, *298*, 199 –209.

Sherman, S.M., & Guillery, R.W. (2011). Distinct functions for direct and transthalamic corticocortical connections. *J. Neurophysiol.*, *106*, 1068-1077.

Shirvalkar, P., Seth, M., Schiff, N. D., & Herrera, D. G. (2006). Cognitive enhancement with central thalamic electrical stimulation. *Proceedings of the National Academy of Sciences*, *103*(45), 17007-17012.

Starzl, T. E., & Magoun, H. W. (1951). Organization of the diffuse thalamic projection system. *Journal of neurophysiology*, *14*(2), 133.

Steriade M., Jones E.G. & McCormick D.A. (1997). Thalamus, Elsevier Amsterdam.

Squire, L. R., Amaral, D. G., Zola-Morgan, S., Kritchevsky, M., & Press, G. (1989). Description of brain injury in the amnesic patient NA based on magnetic resonance imaging. *Experimental neurology*, *105*(1), 23-35.

Van der Werf, Y. D., Scheltens, P., Lindeboom, J., Witter, M. P., Uylings, H. B., & Jolles, J. (2003). Deficits of memory, executive functioning and attention following infarction in the thalamus; a study of 22 cases with localised lesions.*Neuropsychologia*, *41*(10), 1330 1344.

Van der Werf Y.D., Witter M.P. & Groenewegen H.J. (2002) The intralaminar and midline nuclei of the thalamus. Anatomical and functional evidence for participation in processes of arousal and awareness. *Brain. Res. Rev.*, *39*, 107–140.

Vertes R.P. (2006) Interactions among the medial prefrontal cortex, hippocampus and midline thalamus in emotional and cognitive processing in the rat. *Neuroscience.*, *142*, 1–20.

Vertes R.P., Hoover W.B., Do Valle A.C., Sherman A. & Rodriguez J.J. (2006) Efferent projections of reuniens and rhomboid nuclei of the thalamus in the rat. *J. Comp. Neurol.*, *499*, 768–796.

Vertes R.P., Hoover W.B., Szigeti-Buck K. & Leranth C. (2007) Nucleus reuniens of the midline thalamus: Link between the medial prefrontal cortex and the hippocampus. *Brain Res Bull., 71*, 601–609.

Viana Di Prisco G. & Vertes R.P. (2006). Excitatory actions of the ventral midline thalamus (rhomboid/reuniens) on the medial prefrontal cortex in the rat. *Synapse., 60*, 45–55.

Wang, G.W. & Cai, J.X. (2006). Disconnection of the hippocampal-prefrontal cortical circuits impairs spatial working memory performance in rats. *Behav. Brain Research, 175*, 329-336.

Winocur, G., Oxbury, S., Roberts, R., Agnetti, V., & Davis, C. (1984). Amnesia in a patient with bilateral lesions to the thalamus. *Neuropsychologia, 22*(2), 123-143.

Wilson, C. R., Gaffan, D., Browning, P. G., & Baxter, M. G. (2010). Functional localization within the prefrontal cortex: missing the forest for the trees? *Trends in neurosciences*, *33*(12), 533-540.

Wyder, M. T., Massoglia, D. P., & Stanford, T. R. (2003). Quantitative assessment of the timing and tuning of visual-related, saccade-related, and delay period activity in primate central thalamus. *Journal of neurophysiology*, *90*(3), 2029-2052.

Xu, W., Cormier, R., Fu, T., Covey, D. F., Isenberg, K. E., Zorumski, C. F., & Mennerick, S. (2000). Slow death of postnatal hippocampal neurons by GABAA receptor overactivation. *The Journal of Neuroscience*, *20*(9), 3147-3156.

Yoon, T., Okada, J., Jung, M.W. & Kim, J.J. (2008). Prefrontal cortex and hippocampus subserve different components of working memory in rats. *Learn. Mem., 15*, 97-105

Zipser, D., Kehoe, B., Littlewort, G., & Fuster, J. (1993). A spiking network model of short-term active memory. *J. Neurosci., 13*(8), 3406-3420.

Zola-Morgan S. & Squire L.R. (1985). Medial temporal lesions in monkeys impair memory on a variety of tasks sensitive to human amnesia. *Behav. Neurosci., 99*, 22–34.

APPENDIX A

Tables

Subject #	Hemisphere	AP	ML	DV
15	R	+7.0	+1.5	+4.0
61	L	+6.7	+1.0	+5.4
63	R	+6.5	+1.2	+5.4
67	R	+6.7	+1.0	+4.4
73	L	+7.0	+1.2	+4.5

Table 1: Stereotaxic coordinates of Inactivation cannula placement. All coordinates are in millimeters, with AP and DV relative to the interaural line.

Subject #	Hemisphere	AP	ML	DV
15	R	+2.8	+1.5	+4.9
61	L	+3.5	+1.4	+6.4
63	R	+3.2	+0.8	+5.8
67	R	+3.5	+0.6	+4.4
73	L	+4.4	+1.0	+5.0

Table 2: Stereotaxic coordinates of tetrode endpoint lesions. All coordinates are in millimeters with AP relative to Bregma and DV relative to the interaural line.

APPENDIX B

Figures

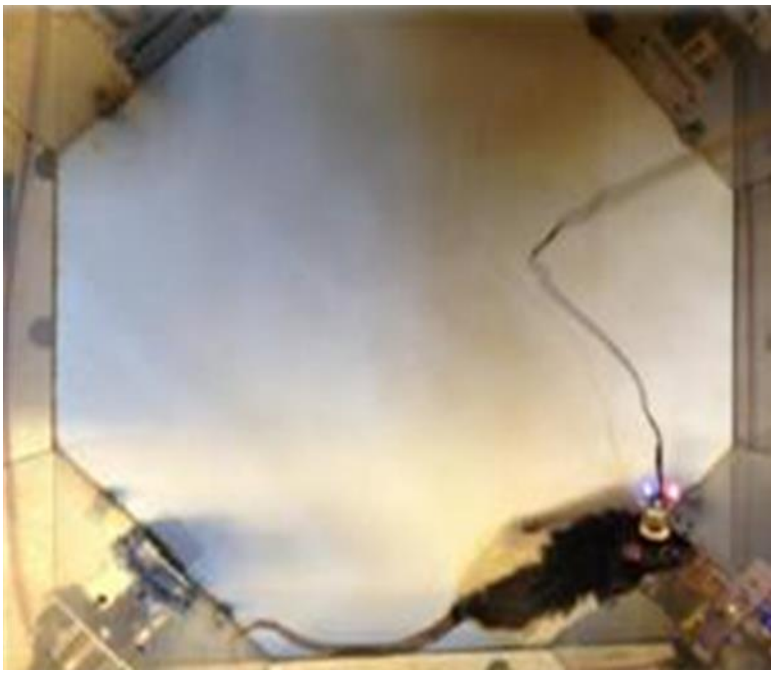

Figure 1: Subject being recorded in operant chamber during DNMTP task.

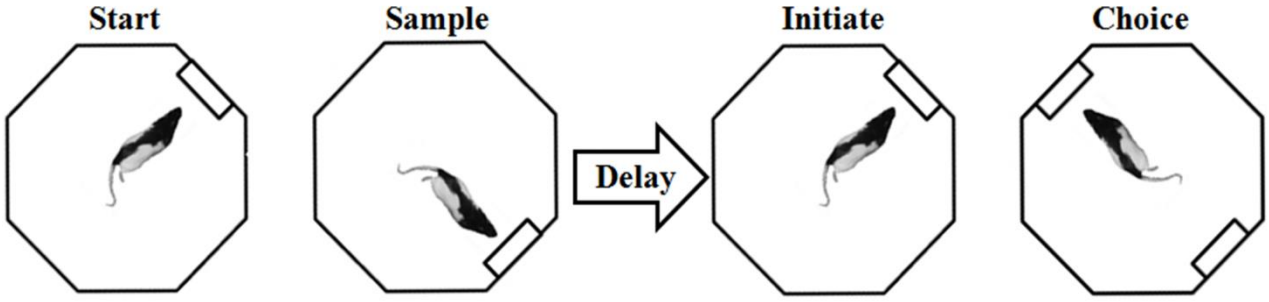

Figure 2: Diagram of DNMTP task phases.

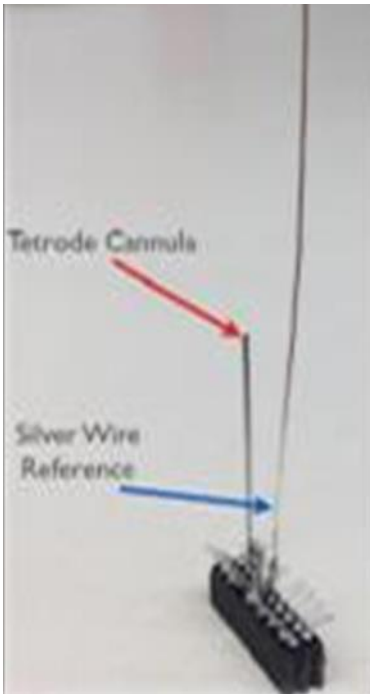

Figure 3: Recording array, before being set in acrylic base and mounted to feet.

Figure 4: Subject with implanted recording array.

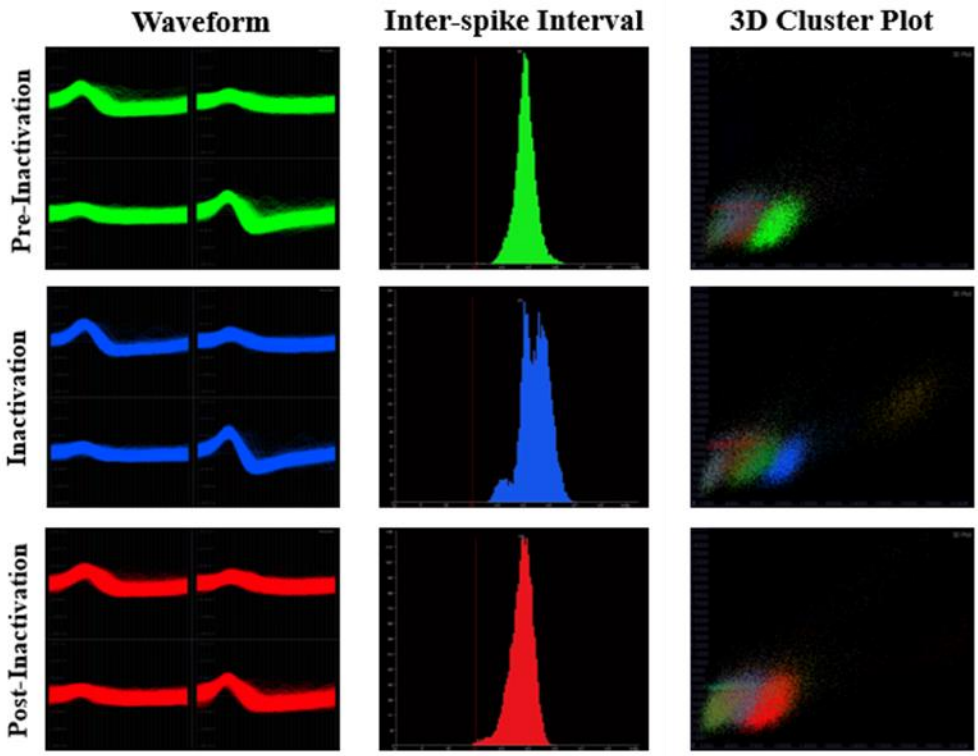

Figure 5: Single cell identified across 3 consecutive days by waveform, ISI histogram, and 3D cluster plot.

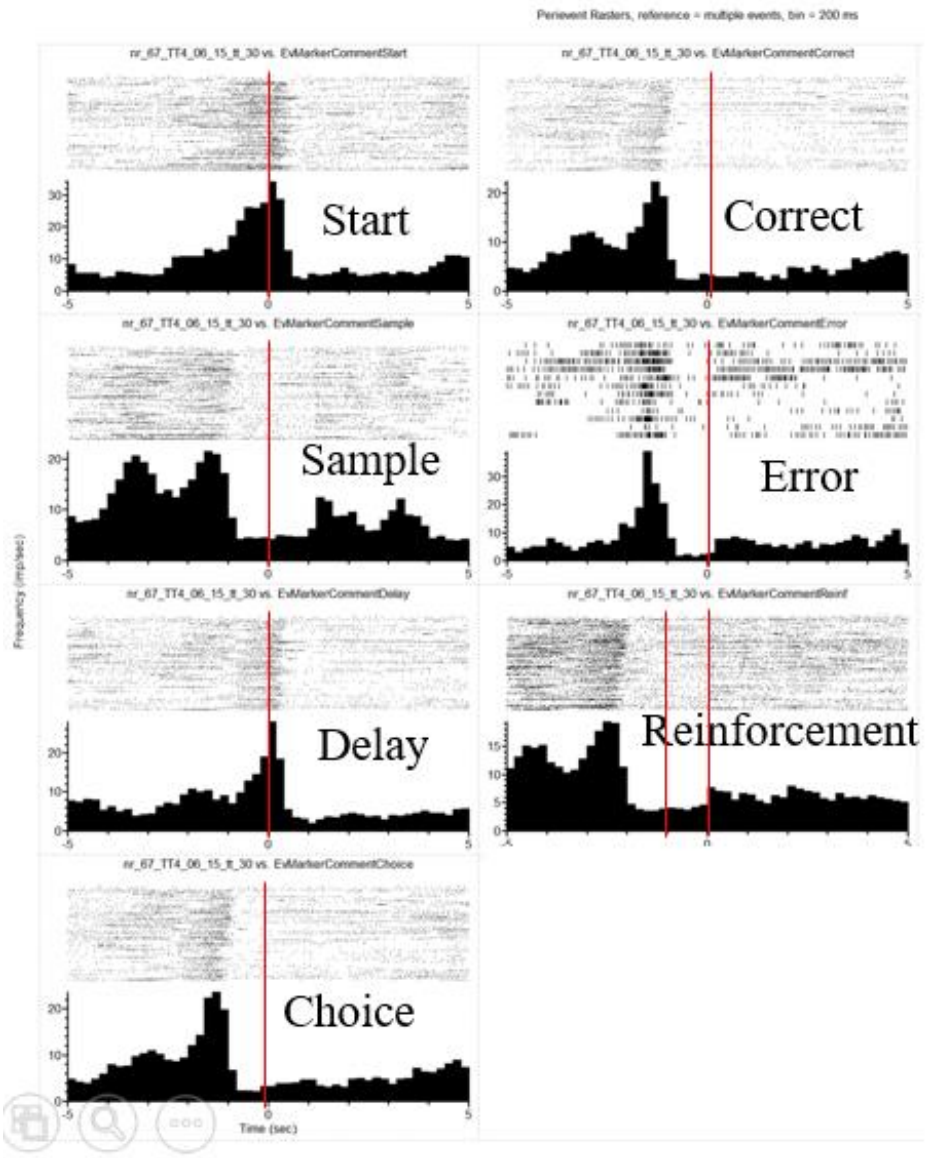

Figure 6: Example of raster plot and PETH for a base lever cell.

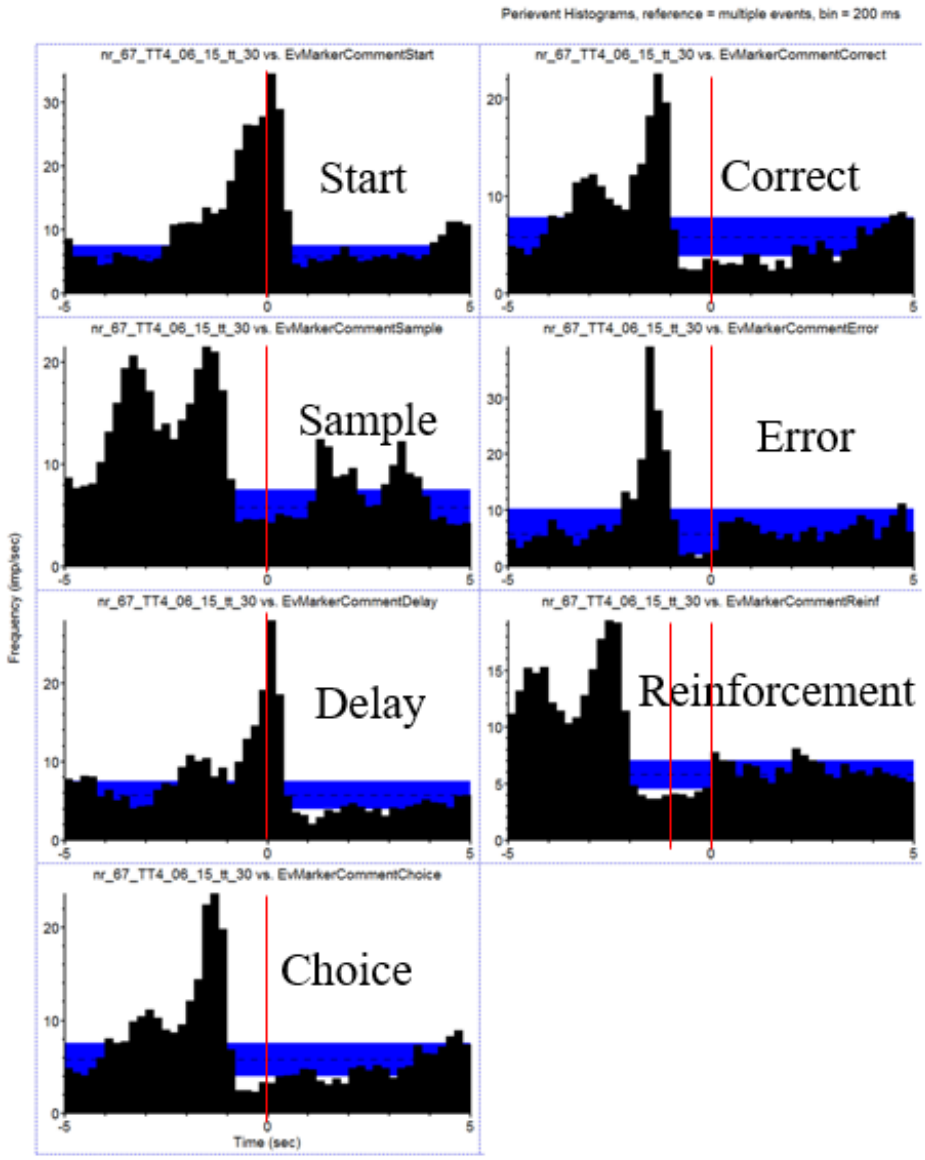

Figure 7: Example of PETHs with 99% confidence interval illustrated for a base lever cell.

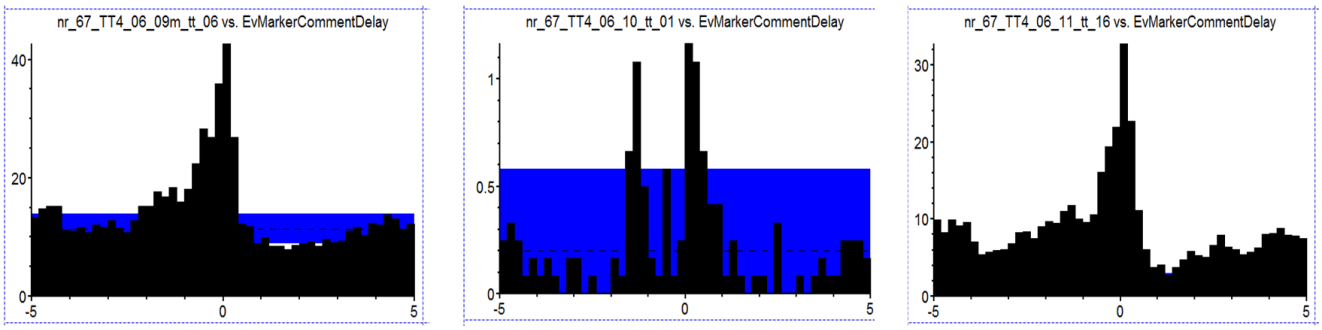

Figure 8: Example of PETH with 99% confidence interval illustrated for the same base lever cell's end-of-delay lever press window on days 1, 2, and 3 of the inactivation sequence.

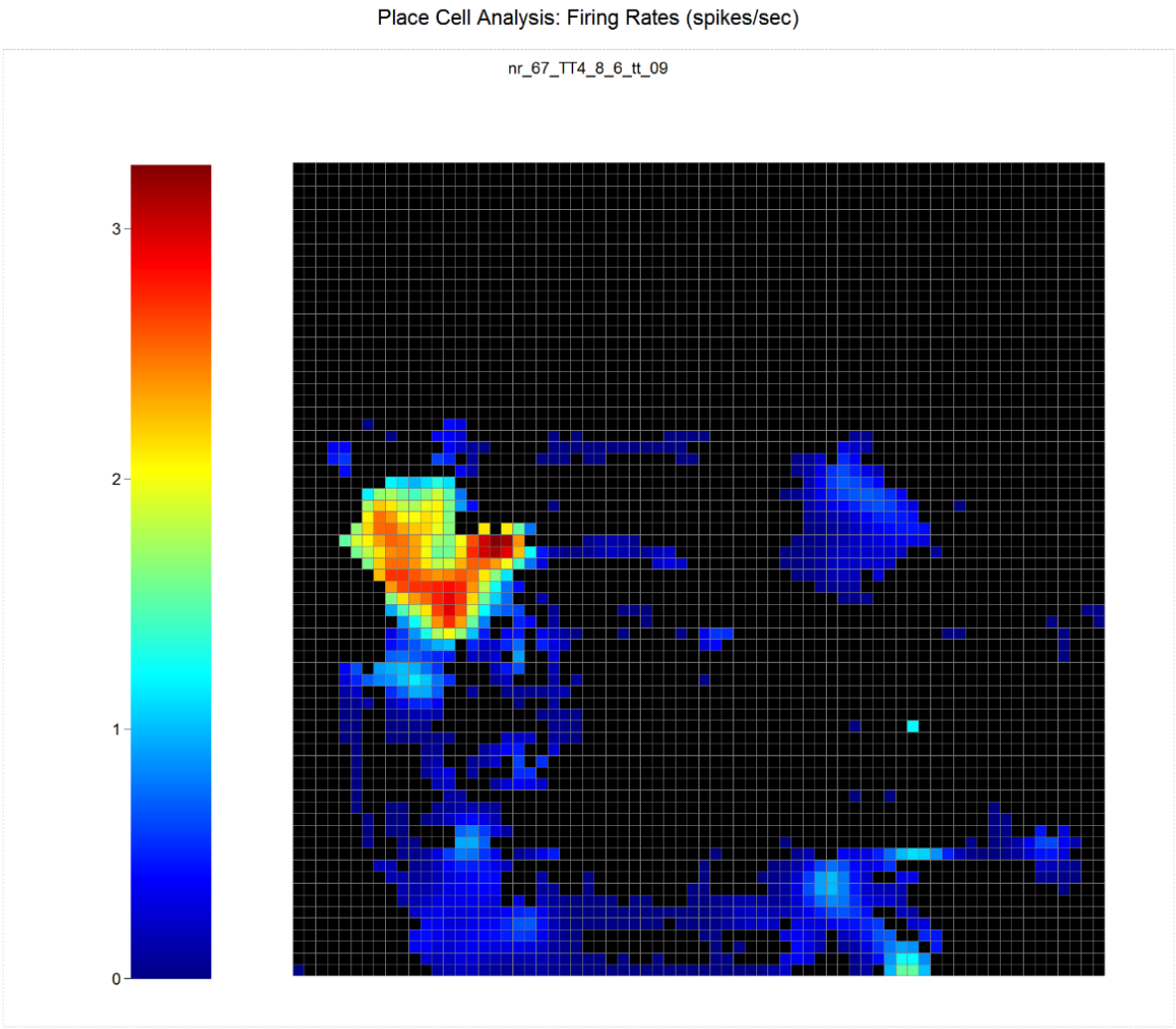

Figure 9: Sample spatial heat map demonstrating location-specific activity of a reinforcement anticipation cell with activity specific to a single reinforcement location.

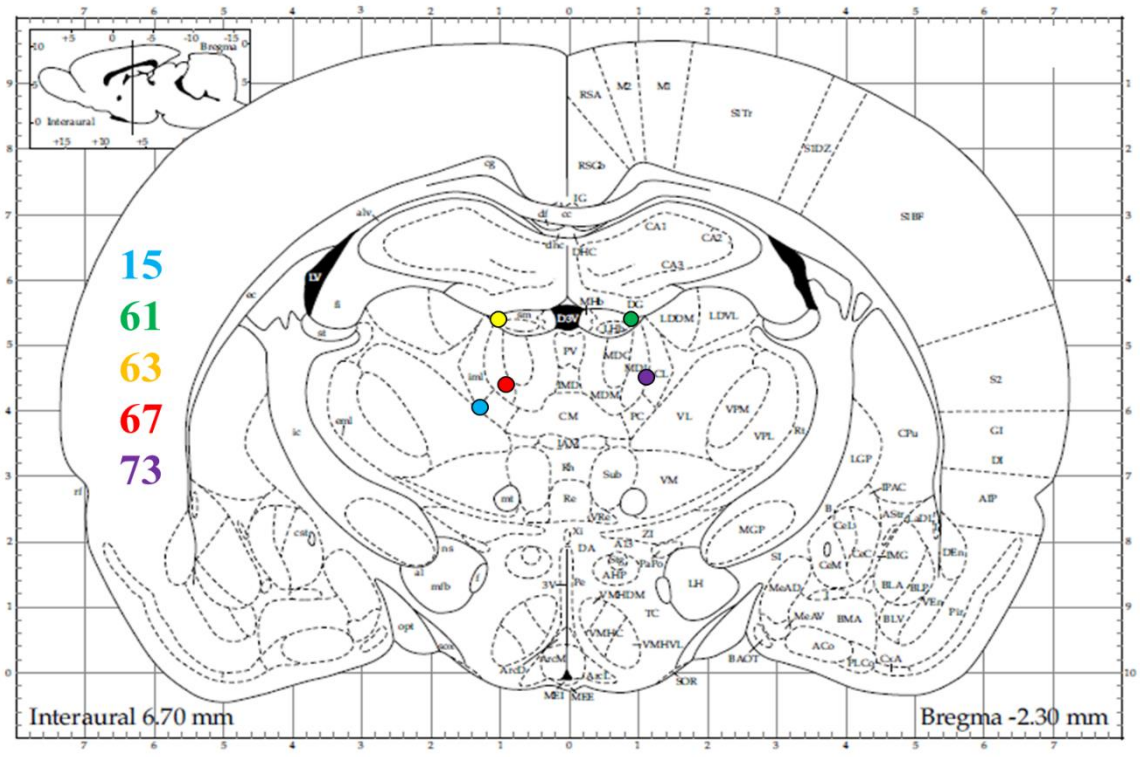

Figure 10: Approximate location of injection sites. Sites are color coded by subject numbers, which are shown on the left.

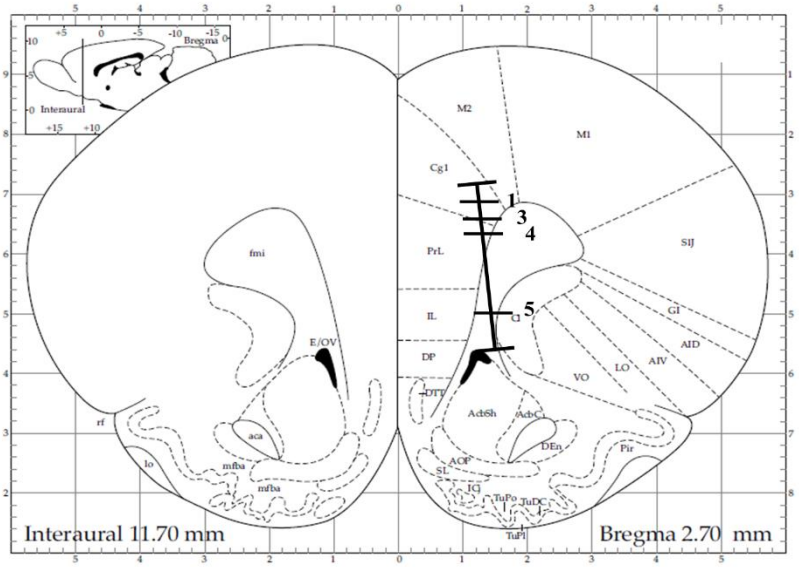

Figure 11: Recording track for subject 15. Depth at all analyzed inactivation days marked with numbered hash marks.

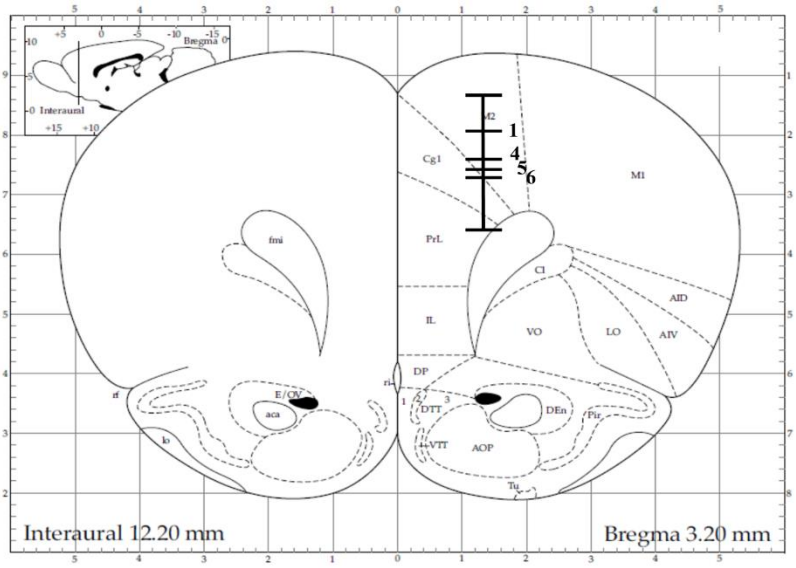

Figure 12: Recording track for subject 61. Depth at all analyzed inactivation days marked with numbered hash marks.

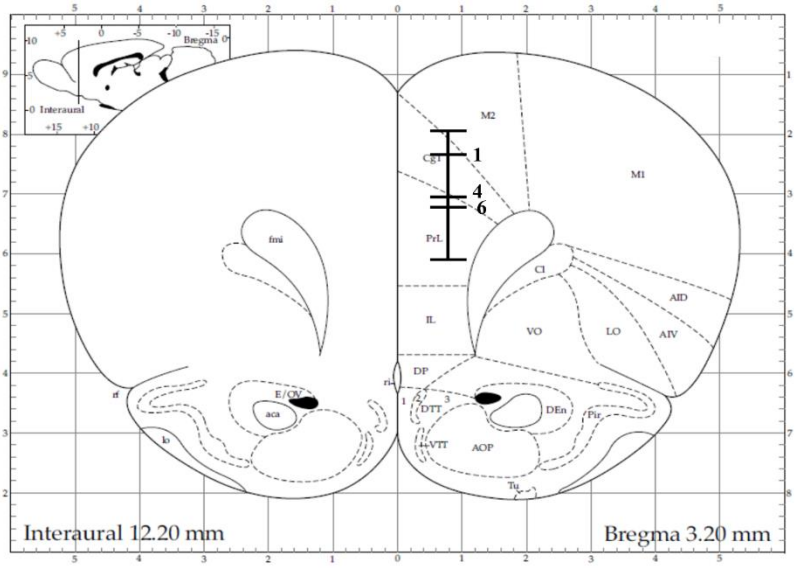

Figure 13: Recording track for subject 63. Depth at all analyzed inactivation days marked with numbered hash marks.

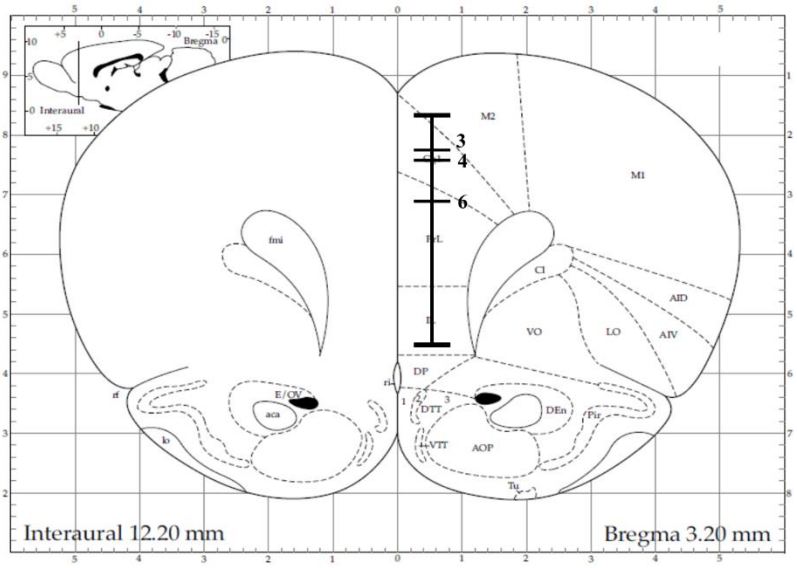

Figure 14: Recording track for subject 67. Depth at all analyzed inactivation days marked with numbered hash marks.

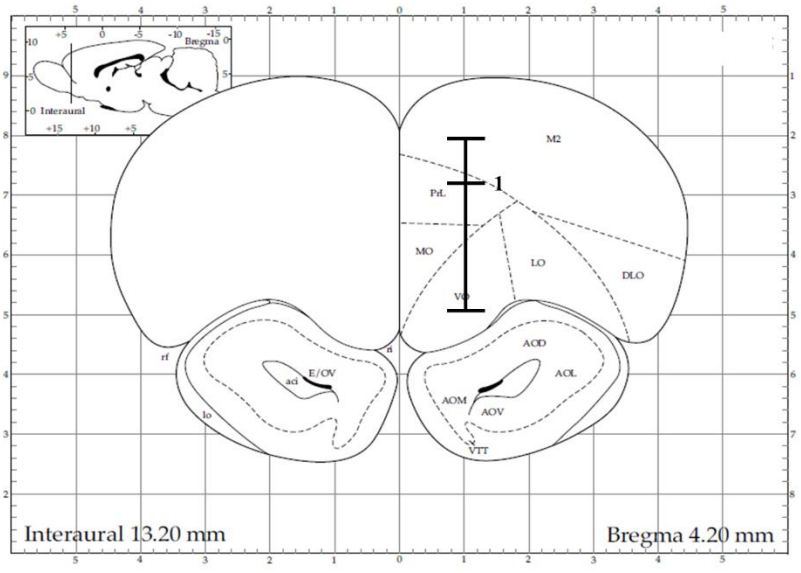

Figure 15: Recording track for subject 73. Depth at first inactivation day marked with number 1 hashmark. This was the only inactivation sequence from which cells were tracked and analyzed.

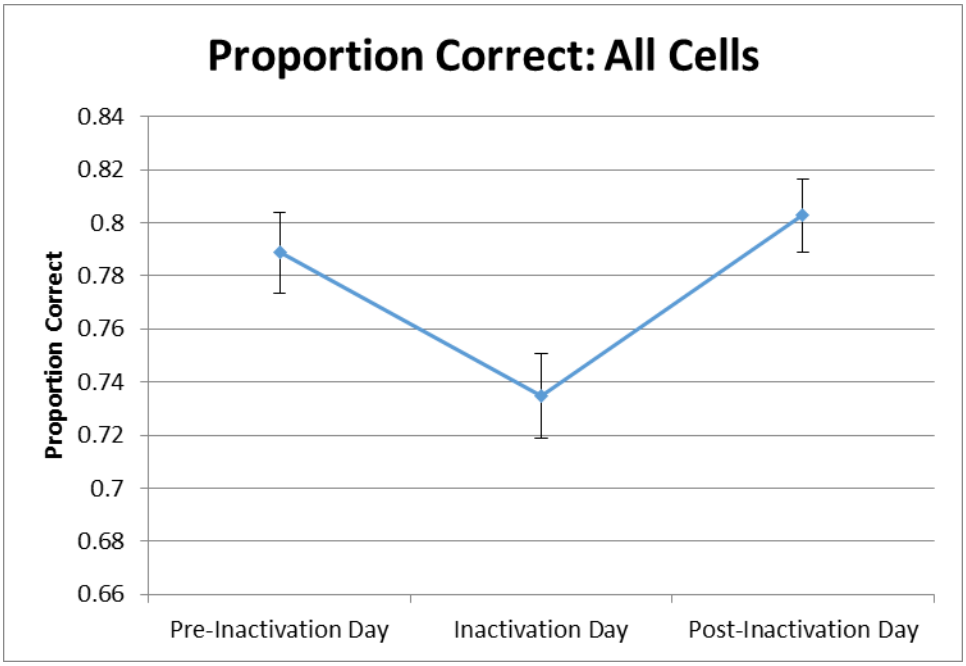

Figure 16: Graph showing the proportion of correct responses significantly impaired by inactivation when all cells are analyzed.

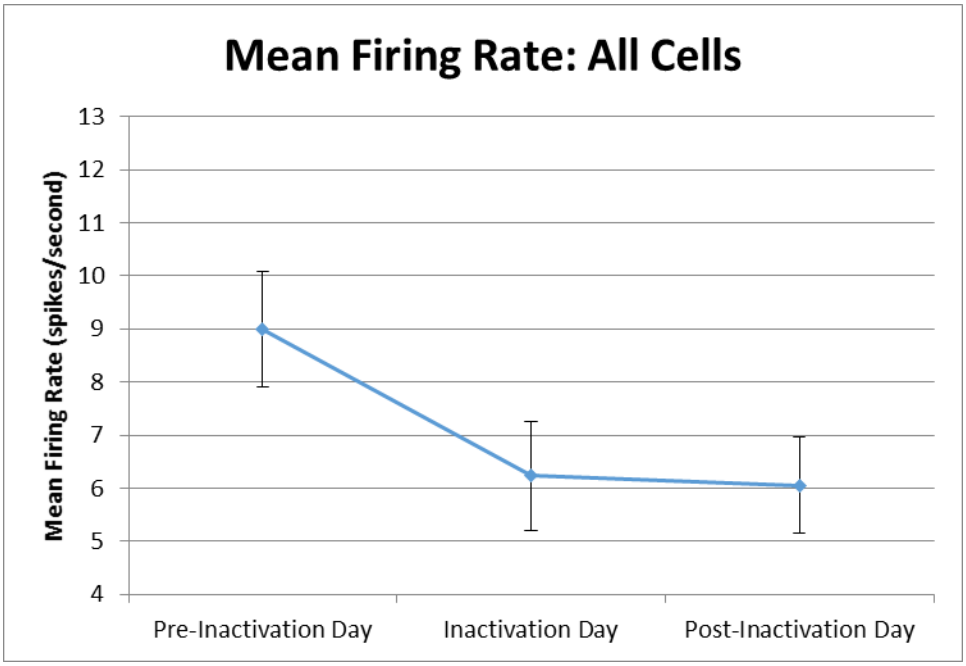

Figure 17: Graph showing significant effect of inactivation on mean firing rate when all cells are analyzed. Day 3 does not differ significantly from day 2.

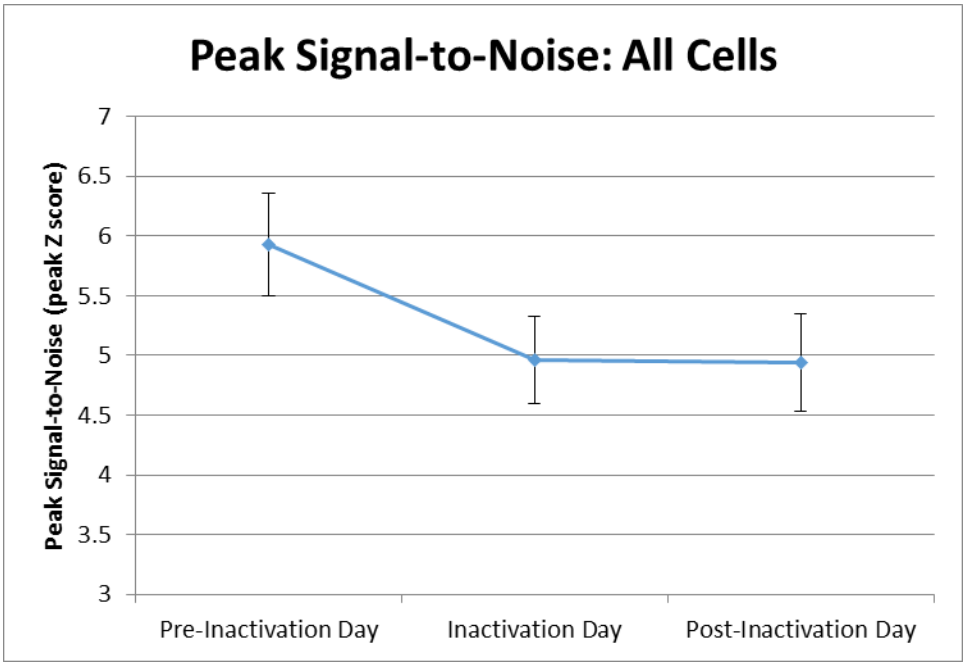

Figure 18: Graph showing significant effect of inactivation on event-specific activity when all cells are analyzed. Day 3 does not differ significantly from day 2.

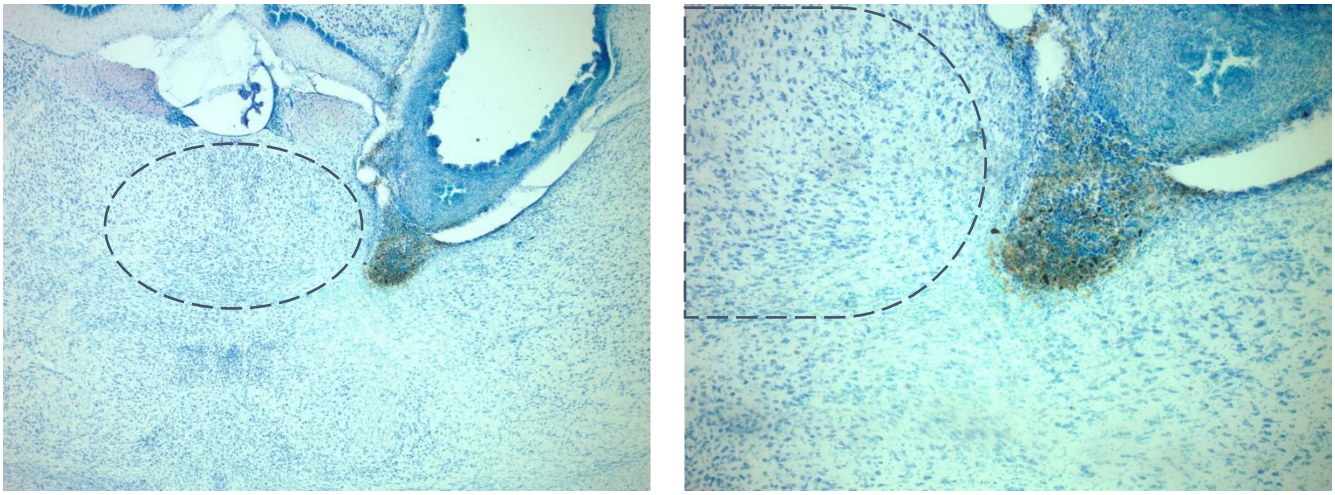

Figure 19: Slide photographs showing hemosiderin deposits surrounding the injection site in subject 67, MD nucleus adjacent to cannula entry outlined (Left slide at 4x magnification; Right slide at 10x magnification).

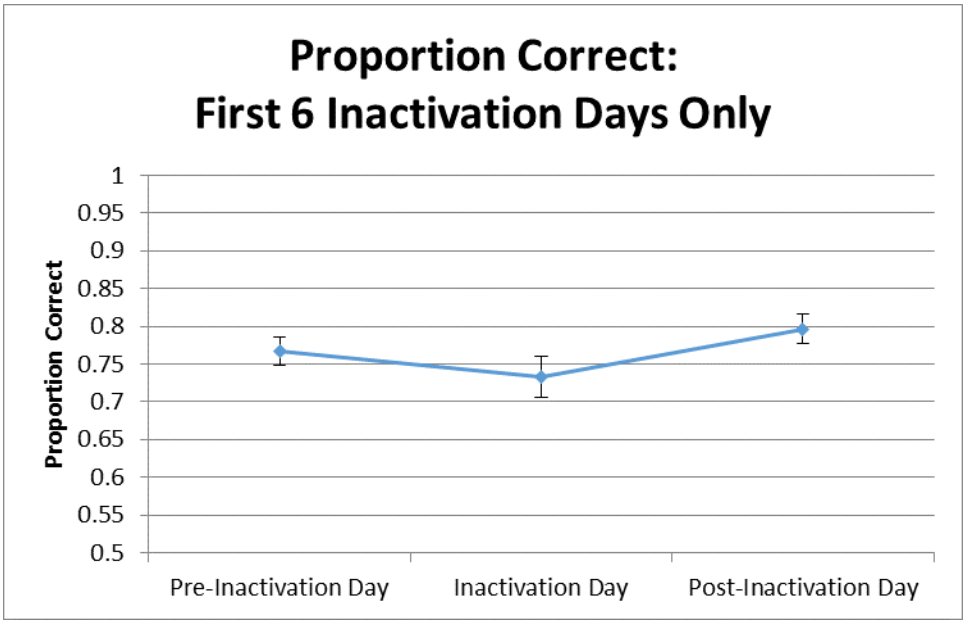

Figure 20: Graph showing the proportion of correct responses not significantly affected by inactivation when inactivation sequences past the sixth are excluded.

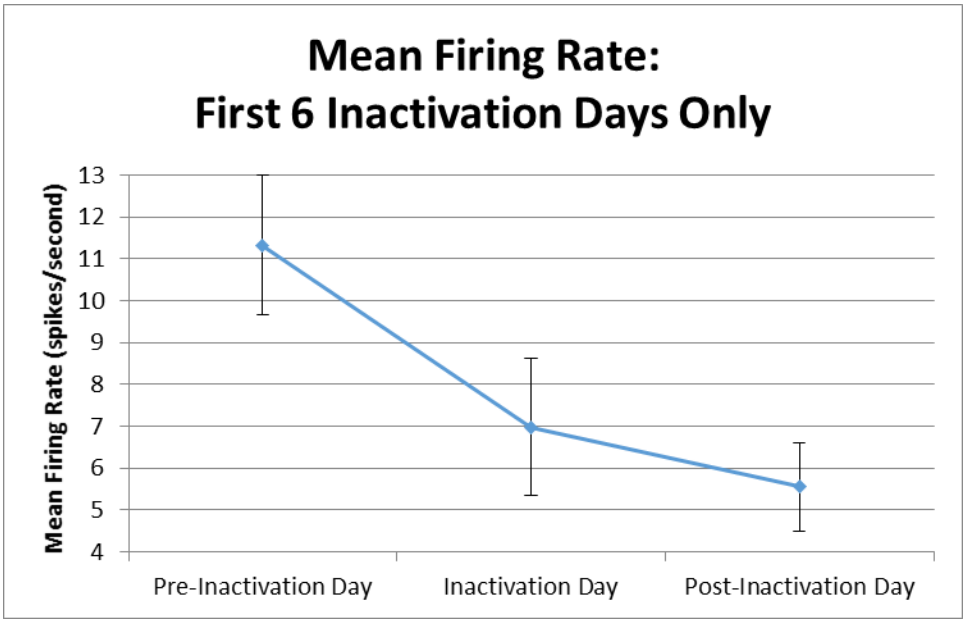

Figure 21: Graph showing mean firing rate not significantly affected by inactivation when inactivation sequences past the sixth are excluded.

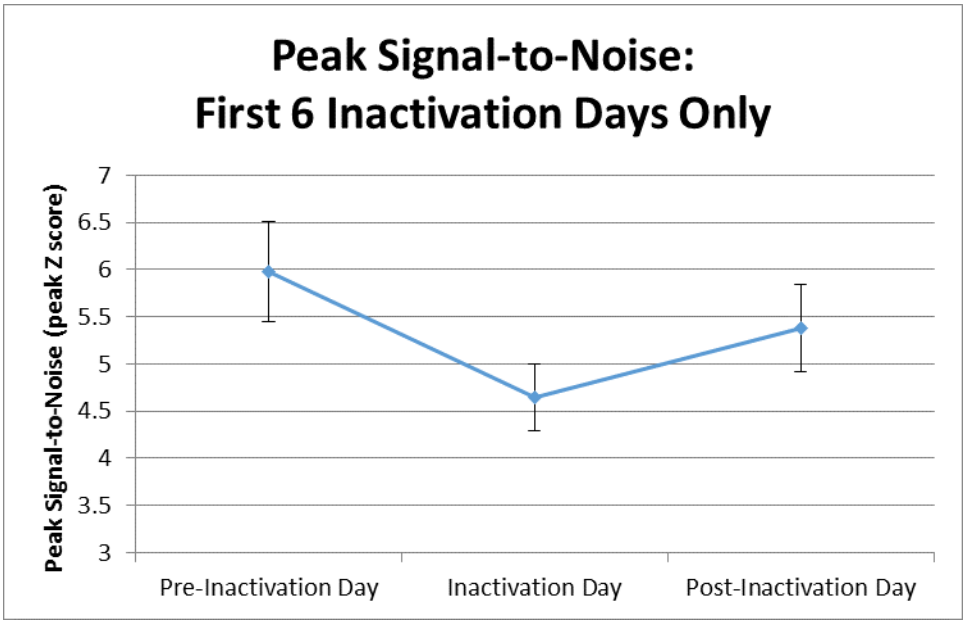

Figure 22: Graph showing significant decrease in event-specific activity produced by inactivation. Lack of significant change from days 1 to 3 indicates recovery of event-related firing properties, supported by significant quadratic fit.

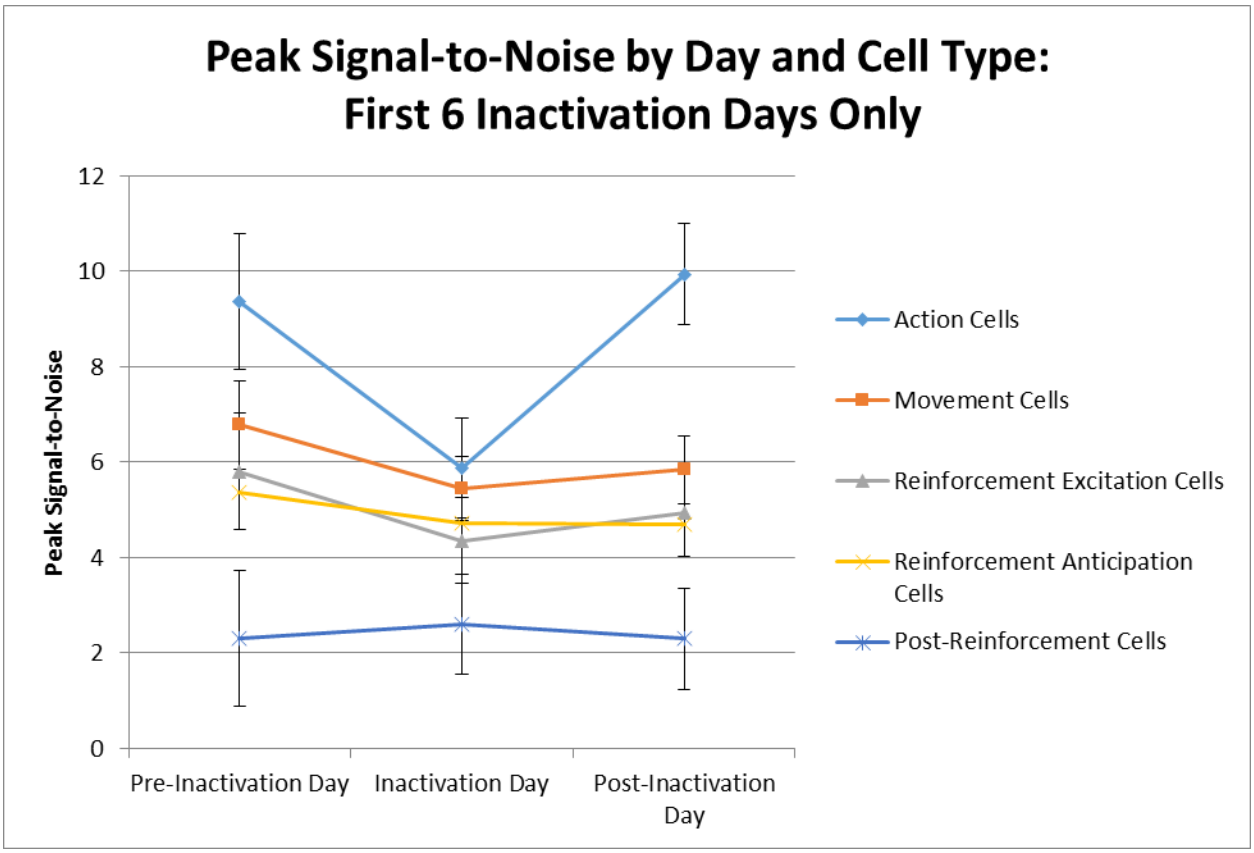

Figure 23: Graph showing interaction of cell type with inactivation on event-specific activity. Interactions are not significant, but effect approached significance for action related cells.

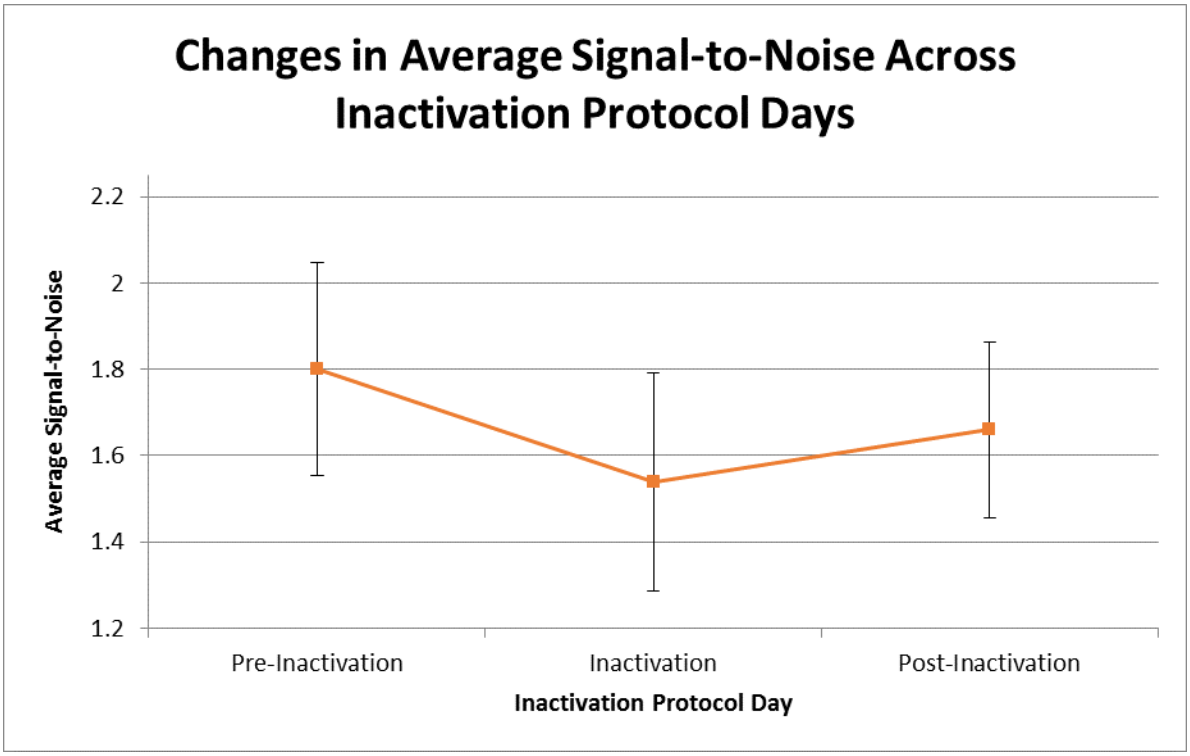

Figure 24: Graph showing non-significant changes in average signal-to-noise across three day inactivation protocol.

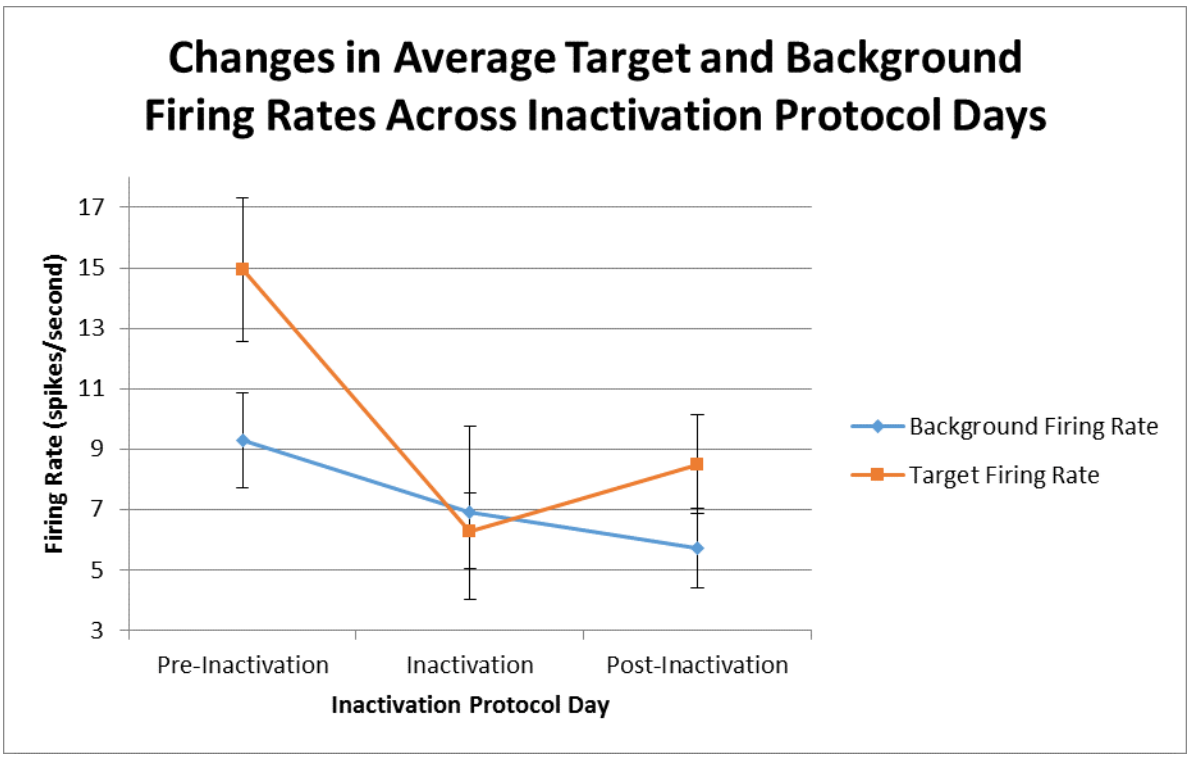

Figure 25: Graph showing changes in average target firing rate and average background firing rate across three day inactivation protocol. Only average target firing rate is significantly affected.

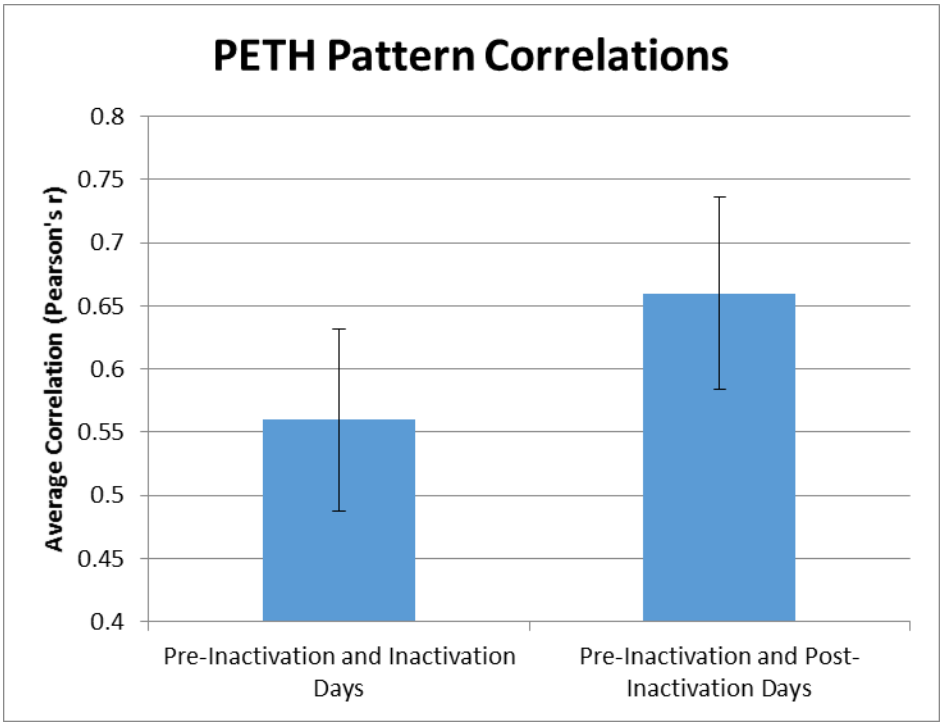

Figure 26: Graph showing comparison of correlations between PETH data from inactivation days. Correlation between pre- and post-inactivation PETH data is significantly stronger than correlation between Pre-inactivation and inactivation data.

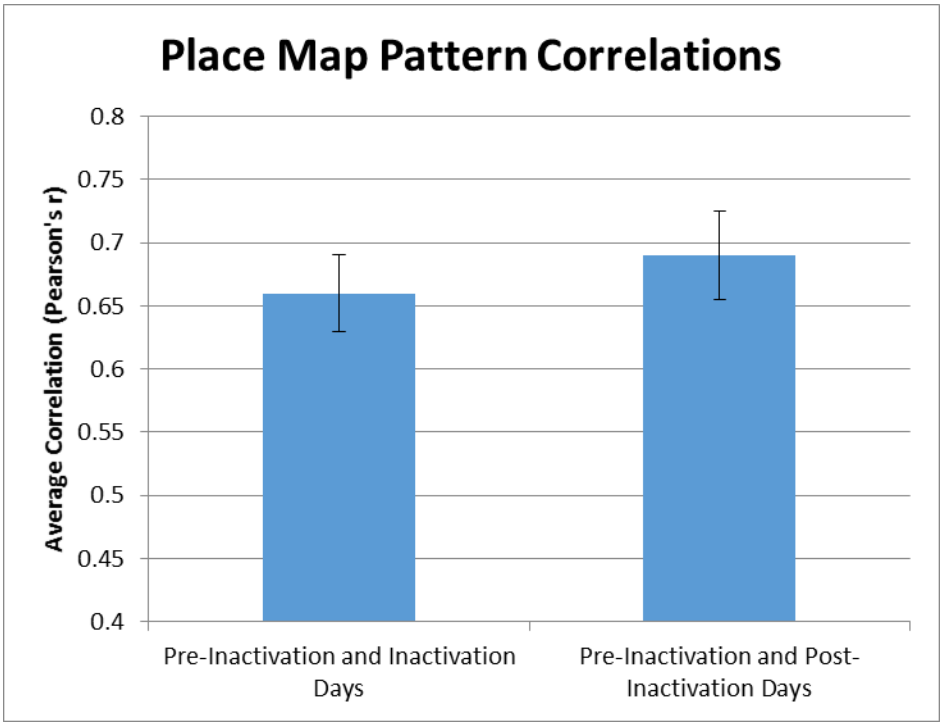

Figure 27: Graph showing comparison of correlation strength between inactivation days for all cells in analysis. No significant difference found.

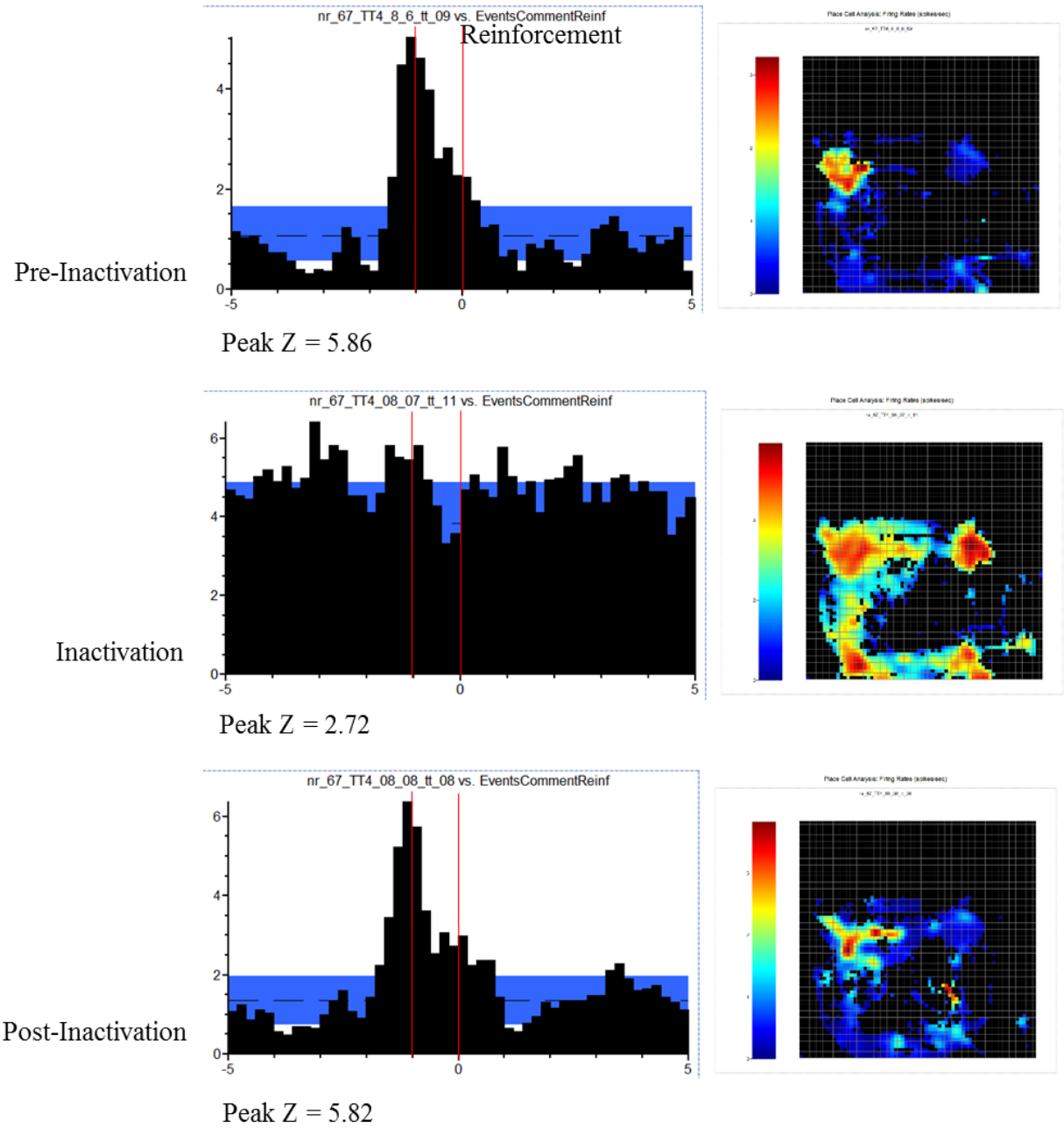

Figure 28: Sample PETHs and spatial heat maps from a reinforcement anticipation cell with location-specific activity before, during and after thalamic inactivation.

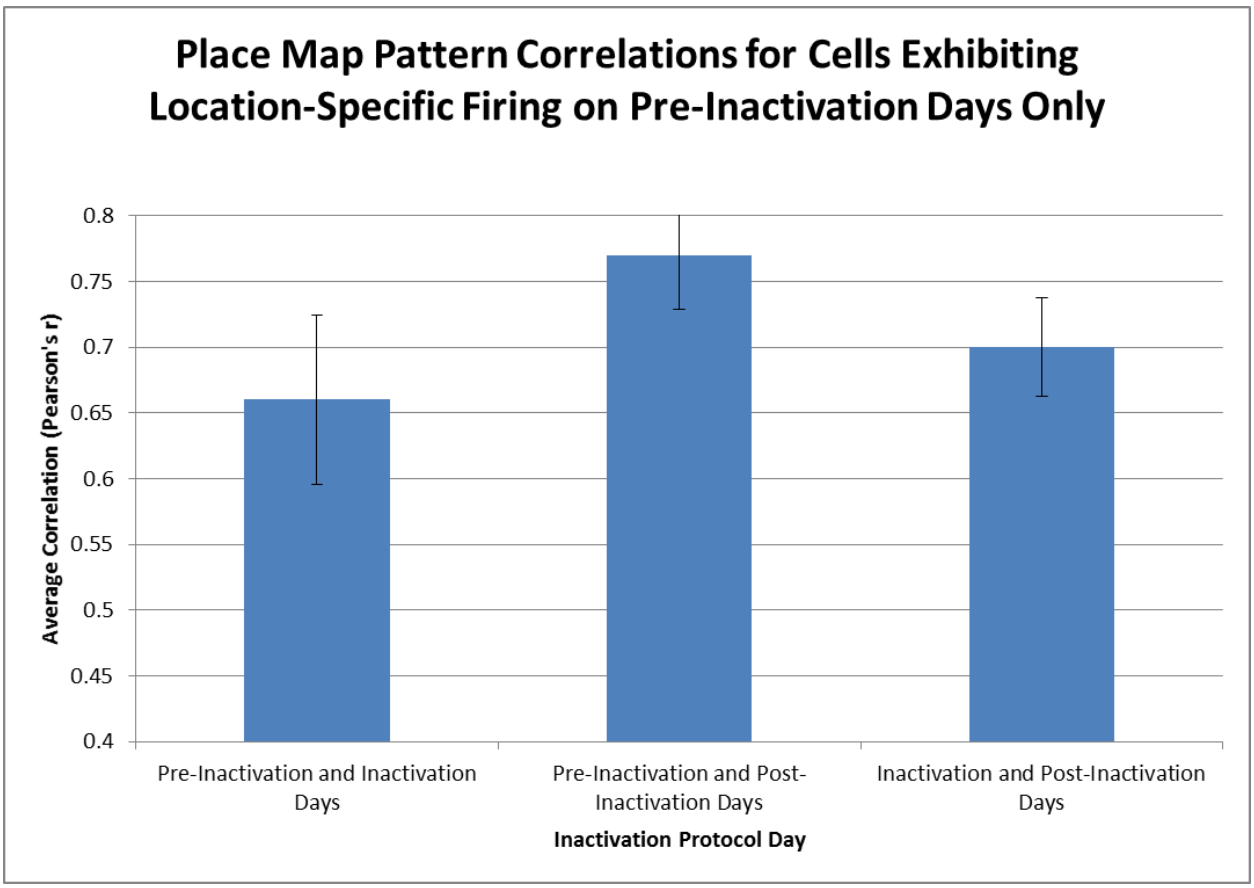

Figure 29: Graph showing correlations between location-specific firing patterns on each inactivation day. Pre- and post-inactivation correlation is significantly stronger than the other two comparisons.

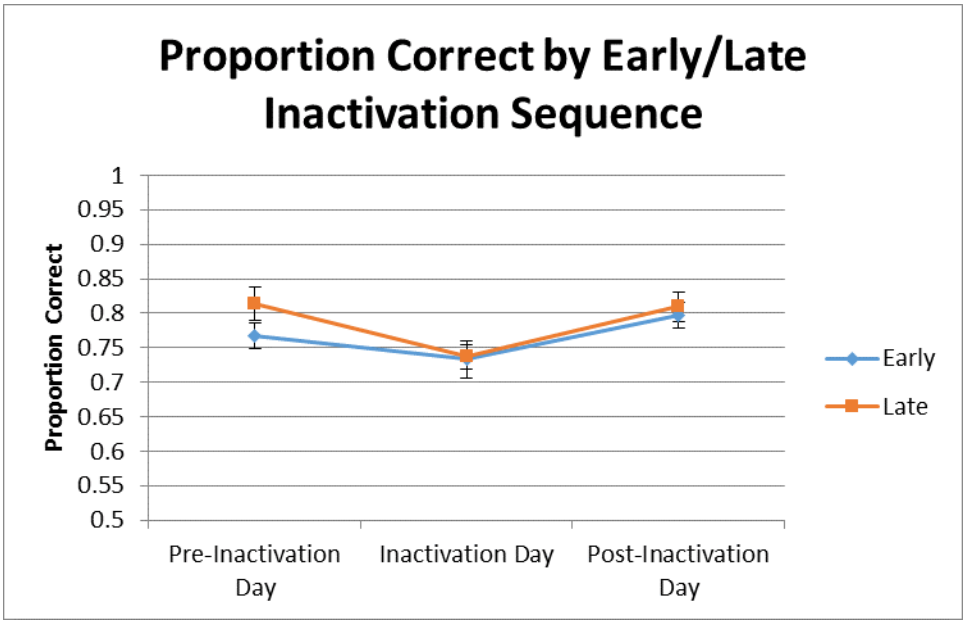

Figure 30: Graph showing effect of inactivation on proportion of correct responses for early and late inactivation groups separately. Only late inactivation group shows significant performance deficit during inactivation.

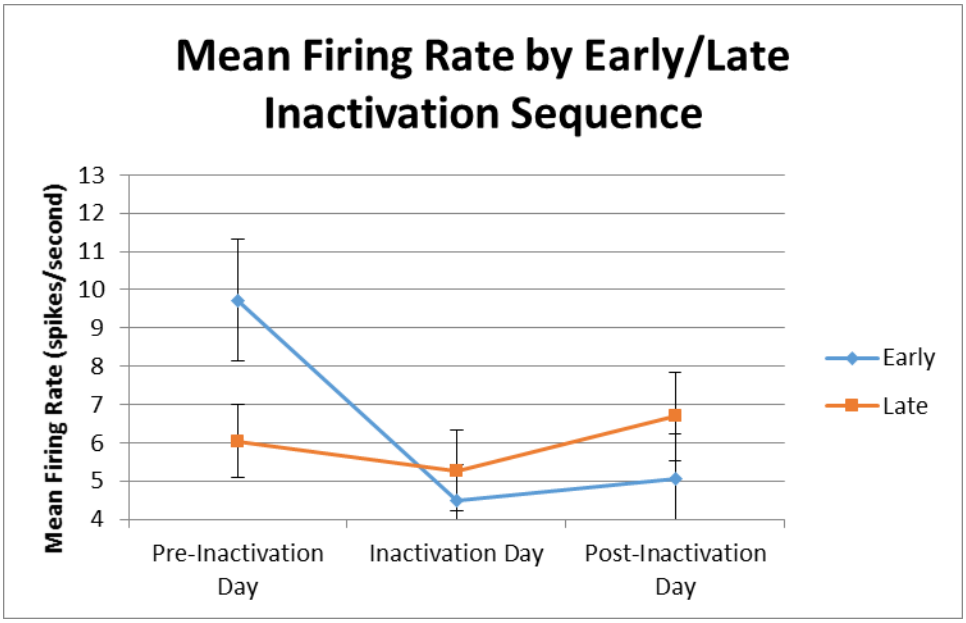

Figure 31: Graph showing non-significant effect of inactivation on mean firing rate for early and late inactivation groups separately. Mean firing rate was lower overall on pre-inactivation days within the late inactivation group only.

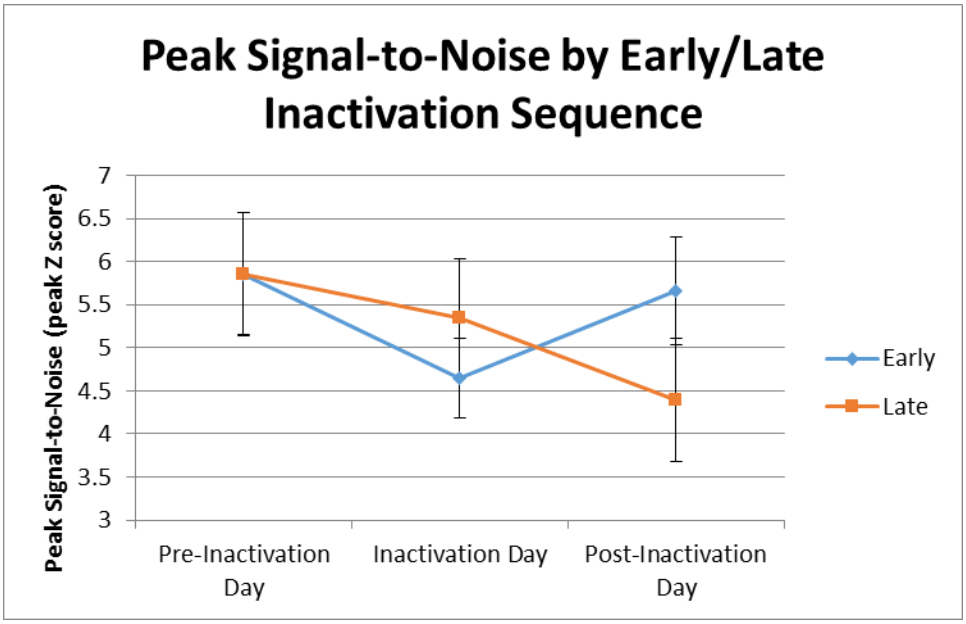

Figure 32: Graph showing effect of inactivation on peak signal-to-noise for early and late inactivation groups separately. Only early inactivation group shows significant effect of inactivation.

APPENDIX C

University *of* New Hampshire

Research Integrity Services, Service Building
51 College Road, Durham, NH 03824-3585
Fax: 603-862-3564

20-Oct-2014

Mair, Robert G
Psychology, McConnell Hall
Durham, NH 03824

IACUC #: 130301
Project: Effects of Thalamic Inactivation on Memory Coding Properties of Prefrontal Neurons in the Rat
Category: D
Modification Approval Date: 14-Oct-2014
Annual Approval Expiration Date: 21-Mar-2015
Protocol Three-Year Approval Expiration Date: 21-Mar-2016

The Institutional Animal Care and Use Committee (IACUC) has reviewed and approved the requested modification to the protocol for this study:

Transfer of 4 animals from #130607

If you have any questions, please contact either Dean Elder at 862-4629 or Julie Simpson at 862-2003.

For the IACUC,

Jill A. McGaughy, Ph.D.
Chair

cc: File

APPENDIX D

Supplemental Data Analyses

In order to assess potential differences between early (first six inactivation sequences) and late (sequences seven and higher) inactivation sequences, we conducted mixed-model ANOVAs with day as the repeated measure, and early vs. late inactivation sequence as a between-subject variable.

Task Performance. A mixed-model ANOVA with day as the repeated measure, early vs. late inactivation sequence as a between-subject variable, and proportion of correct responses as the dependent variable revealed a significant main effect of day on proportion of correct responses, $F(2,52)=7.27$, $p<.05$. A post-hoc LSD test revealed that the proportion of correct responses was significantly lower on inactivation days ($M=.73$, $SD=.08$) compared to both pre-inactivation days ($M=.79$, $SD=.08$) and post-inactivation days ($M=.80$, $SD=.07$), ps$<.05$. Proportion of correct responses did not differ significantly on pre-inactivation and post-inactivation days, $p>.05$, suggesting that inactivation significantly reduced performance accuracy. The mixed-model ANOVA failed to reveal a significant main effect of inactivation sequence on proportion of correct responses ($F(1,26)=1.00$, $p>.05$), indicating there was no overall difference in task performance between early and late inactivation sequences. Finally, the mixed-model ANOVA failed to reveal a significant interaction between day and inactivation sequence on proportion of correct responses ($F<1$), suggesting that the effect of day on proportion of correct responses did not differ significantly between early and late inactivation sequences. Nevertheless, we conducted repeated-measures ANOVAs to examine the effect of day on proportion of correct responses separately within the early and late inactivation sequence

groups. As reported in the main text, this analysis failed to reach significance within the early inactivation sequence group, $F(2,28)=3.01$, $p>.05$. However, the analyses revealed a significant main effect of day on proportion of correct responses within the late inactivation sequence group, $F(2,24)=4.82$, $p<.05$. A post-hoc LSD test revealed that within the late inactivation sequence group, the proportion of correct responses was significantly lower on inactivation days ($M=.74$, $SD=.06$) compared to both pre-inactivation days ($M=.81$, $SD=.09$) and post-inactivation days ($M=.81$, $SD=.08$), ps$<.05$. Proportion of correct responses did not differ significantly on pre-inactivation and post-inactivation days, $p>.05$ (See Figure 30).

Mean Firing Rate. A mixed-model ANOVA with day as the repeated measure, early vs. late inactivation sequence as a between-subject variable, and mean firing rate as the dependent variable revealed a significant main effect of day on mean firing rate, $F(2,84)=5.24$, $p<.05$. A post-hoc LSD test revealed that the mean firing rate was significantly lower on inactivation days ($M=4.90$, $SD=4.70$) than on pre-inactivation days ($M=7.80$, $SD=6.23$). Mean firing rate on post-inactivation days ($M=5.92$, $SD=5.48$) did not differ significantly from either pre-inactivation or inactivation days, ps$>.05$, indicating only partial recovery following inactivation. The mixed-model ANOVA failed to reveal a significant main effect of inactivation sequence on mean firing rate ($F<1$), indicating there was no overall difference in mean firing rate between early and late inactivation sequences. Finally, the mixed-model ANOVA revealed a significant interaction between day and inactivation sequence on mean firing rate ($F(2,84)=4.55$, $p<.05$), suggesting that the effect of day on mean firing rate differed significantly between early and late inactivation sequences. To examine this interaction, we conducted repeated-measures ANOVAs to determine the effect of day on mean firing rate separately within the early and late inactivation sequence groups. As reported in the main text, there was a significant effect of day on mean

firing rate within the early inactivation sequence group, $F(2,40)=6.85$, $p<.05$. However, the analyses failed to reveal a significant effect of day on mean firing rate within the late inactivation sequence group ($F<1$), suggesting cells responded differently to inactivation in animals which received a greater number of injections. To examine this further, we conducted a series of independent t-tests to compare the mean firing rate of the early and late inactivation sequence groups on each inactivation day. These analyses revealed that mean firing rate did not differ significantly between early and late inactivation sequence groups on inactivation days and post-inactivation days (ts<1), but that on pre-inactivation days mean firing rate was significantly higher in the early inactivation sequence group (M=9.73, SD=7.26) compared to the late inactivation sequence group (M=6.04, SD=4.61), $t(42)=2.03$, $p<.05$) (See Figure 31). This suggests that the interaction of inactivation sequence and day on mean firing rate was driven by the low starting mean firing rate seen in the late inactivation sequence group.

Peak signal-to-noise. A mixed-model ANOVA with day as the repeated measure, early vs. late inactivation sequence as a between-subject variable, and peak signal-to-noise as the dependent variable revealed only a marginally significant main effect of day on peak signal-to-noise, $F(2,84)=2.32$, $p=.11$. A post-hoc LSD test revealed that peak signal-to-noise was marginally lower on inactivation days (M=5.01, SD=2.79) compared to both pre-inactivation days (M=5.86, SD=3.30) and post-inactivation days (M=4.99, SD=3.20), ps<.09. Peak signal-to-noise did not differ significantly on pre-inactivation and post-inactivation days, $p>.05$. The mixed-model ANOVA failed to reveal a significant main effect of inactivation sequence on peak signal-to-noise ($F<1$), indicating there was no overall difference in peak signal-to-noise between early and late inactivation sequences. Finally, the mixed-model ANOVA revealed a marginally significant interaction between day and inactivation sequence on peak signal-to-noise,

$F(2,84)=2.38$, $p=.10$. To examine this interaction, we conducted repeated-measures ANOVAs to determine the effect of day on peak signal-to-noise separately within the early and late inactivation sequence groups. This analysis revealed only a marginally significant effect of day on peak signal-to-noise within the early inactivation sequence group, $F(2,40)=2.85$, $p=.07$. Post-hoc LSD tests revealed that, within the early inactivation sequence group, peak signal-to-noise was significantly lower on inactivation days ($M=4.65$, $SD=2.10$) compared to pre-inactivation days ($M=5.86$, $SD=3.23$), $p<.05$. Peak signal-to-noise on post-inactivation days ($M=5.66$, $SD=2.88$) was marginally higher than on inactivation days ($p=.06$), and did not differ significantly from pre-inactivation days, $p>.05$. As reported in the main text, a planned quadratic contrast on these means within the early inactivation sequence group was significant, $F(1,20)=7.71$, $p<.05$ and the residual contrast was not significant ($F<1$), suggesting that the means fit the predicted pattern of results within the early inactivation sequence group (i.e., less peak signal-to-noise on inactivation days compared to both pre- and post-inactivation days). The repeated-measures ANOVA examining the impact of day on peak signal-to-noise within the late inactivation sequence group was also marginally significant, $F(2,44)=2.17$, $p=.13$. Post-hoc LSD tests revealed that, within the late inactivation sequence group, peak signal-to-noise was significantly lower on post-inactivation days ($M=4.39$, $SD=3.41$) than on pre-inactivation days ($M=5.85$, $SD=3.44$), $p<.05$. Peak signal-to-noise on inactivation days ($M=5.34$, $SD=3.31$) did not differ significantly from either pre-or post-inactivation days, ps$>.05$. As is apparent from the visual inspection of the means, the planned quadratic contrast on peak signal-to-noise within the late inactivation sequence group was not significant, $F<1$, suggesting the means within the late inactivation sequence group did not fit the predicted pattern of results. While peak signal-to-noise recovered to pre-inactivation day levels within the early inactivation sequence group, peak

signal-to-noise within the late inactivation sequence group not only failed to recover on post-inactivation days, but declined steadily across days (See Figure 32).